Chapter 2

Hydrodynamics and Flow Regimes

It is futile to do with more, what can be done with less.

Occam's razor

INTRODUCTION

In Chapter 1, various technological aspects and conceptual issues relevant to reactor engineering of trickle bed reactors are discussed including the industrial applications and engineering science challenges related to design and scale-up. The importance of multiscale modeling is also discussed in the context of complexities involved in understanding the performance of trickle bed reactors at different scales. It is, however, important and essential to use the accumulated knowledge and wisdom of operating trickle beds to complement and to realize the real benefits of the multiscale modeling. Significant body of experimental data and models are available on various aspects of hydrodynamics, mass and heat transfer, and reactor engineering of trickle bed reactors. Available knowledge on hydrodynamics, flow regimes, and transport parameters in the trickle bed is critically reviewed and presented in a usable form in this chapter. The next chapter (Chapter 3) describes conventional reaction engineering models for trickle bed reactors.

Reaction engineering models (discussed in Chapter 3) based on overall material and energy balances require various design parameters representing hydrodynamics of trickle beds such as liquid holdup, mass and heat transfer coefficients, and axial dispersion. It is essential to establish the relationship of these hydrodynamic parameters with *the key design and operating variables* of the trickle bed reactors. These hydrodynamic parameters are usually obtained from cold flow experiments at much smaller scales than the actual scales employed in industry and the applicability of these at higher scales is often debated. Experimental data used to develop appropriate correlations for establishing relationship with the design and operating parameters are often based on model air−water system and hence their applications to other systems should be done carefully. The development of correlations based on

Trickle Bed Reactors. DOI: 10.1016/B978-0-444-52738-7.10002-6

dimensionless numbers with physical significance and on extensive experimental data has been found to be useful in many cases. This chapter provides comprehensive information on available correlations for the estimation of these parameters useful in designing a trickle bed reactor.

A trickle bed reactor can be visualized as a bed of catalyst particles with interstitial space among them forming a complex pattern of interconnecting and randomly distributed pores. When gas and liquid reactants flow over these catalyst particles, complex interactions between the flowing fluid phases and stationary solid particles lead to different flow patterns or regimes. These flow patterns essentially depend on the packing density, gas and liquid velocities, particle size, and physical properties of the fluid phases. In trickle bed reactors, at least four different flow regimes are recognized (Charpentier, Bakos, & Le Goff, 1971; Charpentier, Prost, & Le Goff, 1969; Fukushima & Kusaka, 1977a, 1977b; Herskowitz & Smith, 1983; Weekman & Myers, 1964). Earlier attempts of developing correlations for the design parameters without considering the differences in flow regimes were not very successful for extrapolation to different systems and scales. It is therefore important to understand the intricacies of different flow regimes, and the ways of identifying prevailing flow regime and transition between them for a specific configuration of the trickle bed reactor at given operating conditions. Various theoretical and experimental methods have been used to investigate different flow regimes in trickle bed reactors (see, for example, Charpentier et al., 1971, 1969; Duduković, 1977; Dudukovic, 2000; Herskowitz & Smith, 1983; Satterfield, 1975). Classification of the flow regimes and their key hydrodynamic characteristics are discussed in the following section. The transition boundaries between different regimes need to be identified accurately since more often than not trickle bed reactors are operated closer to these transition boundaries. The correlations and models for estimating flow regime transition are presented in *Flow Regime Transition* section. Several hydrodynamic and transport parameters such as pressure drop, liquid holdup, wetting of particles, and interphase mass and heat transfer coefficients and interfacial area are considerably affected by the prevailing flow regime. Different methods (models and correlations) for estimating the hydrodynamic and transport parameters in different flow regimes of trickle bed reactors are discussed in *Estimation of Key Hydrodynamic Parameters* section.

FLOW REGIMES

Packed bed reactors are composed of a pore network of complex shapes formed by randomly packed catalyst particles. When fluid is subjected to flow through such a network, it preferably flows through the path which offers least resistance. This usually results in inhomogeneous velocity and phase distribution in the bed. Different flow regimes are observed even in a single-phase flow through packed beds.

For a single-phase flow, at very low flow rates, creeping flow exists for $Re_p < 1$, where Re_p is the particle Reynolds number based on mean velocity in the void space ($Re_p = \rho U_0 d_p/\varepsilon\mu$); the inertial flow regime begins above $Re_p = 10$. This inertial flow regime extends up to $Re_p = 250-350$. With further increase in Reynolds number, the transition flow regime (unsteady flow) occurs up to $Re_p = 900$ (Seguin, Montillet, Comiti, & Huet, 1998). The transition of flow from laminar to turbulent characteristics in the packed beds is difficult to identify and occurs over a range of Reynolds numbers. The occurrence of transition to turbulence regime is a complex function of size and shape of particles and bed packing characteristics. Previous studies (for example, Chhabra, Comiti, & Machac, 2001; Seguin, Montillet, & Comiti, 1998; Seguin et al. 1998) indicate that beyond $Re_p = 350$, flow is dominated by eddies and turbulent-like structures. Seguin et al. (1998) experimentally showed that turbulent flow exists beyond $Re_p = 900$. Jolls and Hanratty (1966) and Latifi, Midoux, Storck, and Gence (1989) reported that transition occurs over the range of $Re_p = 300-400$ ($Re_p = \rho U_0 d_p/\mu$). Based on these studies, it can be assumed that flow becomes completely turbulent beyond a particle Reynolds number of 1000.

When gas and liquid phases are flowing cocurrently downward through a packed bed of solid particles (as in trickle bed reactors), the situation is much more complex compared to the single-phase flow. Most of the trickle bed reactors are operated in a cocurrent manner and hence the discussion here is mainly focused on cocurrent operation. In trickle bed reactors, various flow regimes were observed at different gas and liquid flow rates. Apart from the flow rates of gas and liquid, prevailing flow regime is also a function of parameters such as dimensions of the reactor, size and shape of particles, method of packing, and thermo-physical properties of gas and liquid phases. Broader classification of the two-phase flows in the packed bed reactors is based on the nature of flow of individual phases viz., continuous, semi-continuous, and dispersed flow. Four distinct flow regimes were identified in trickle bed reactors (Chaudhari and Ramachandran (1983):

- Trickle flow regime,
- Pulse flow regime,
- Spray flow regime, and
- Bubbly flow regime.

Names of these flow regimes indicate their typical characteristics which are shown schematically in Fig. 1. Flow characteristics of these regimes are quite distinct and therefore it is important to understand the dominating features of each flow regime. Traditionally, different flow regimes have been studied experimentally by varying either gas or liquid flow rates. At low gas and liquid flow rates, gas–liquid interaction is small and liquid flows in the form of films or rivulets over the packed particles as shown in Fig. 1a. This flow regime is known as trickle flow regime or low interaction regime. At moderate gas and

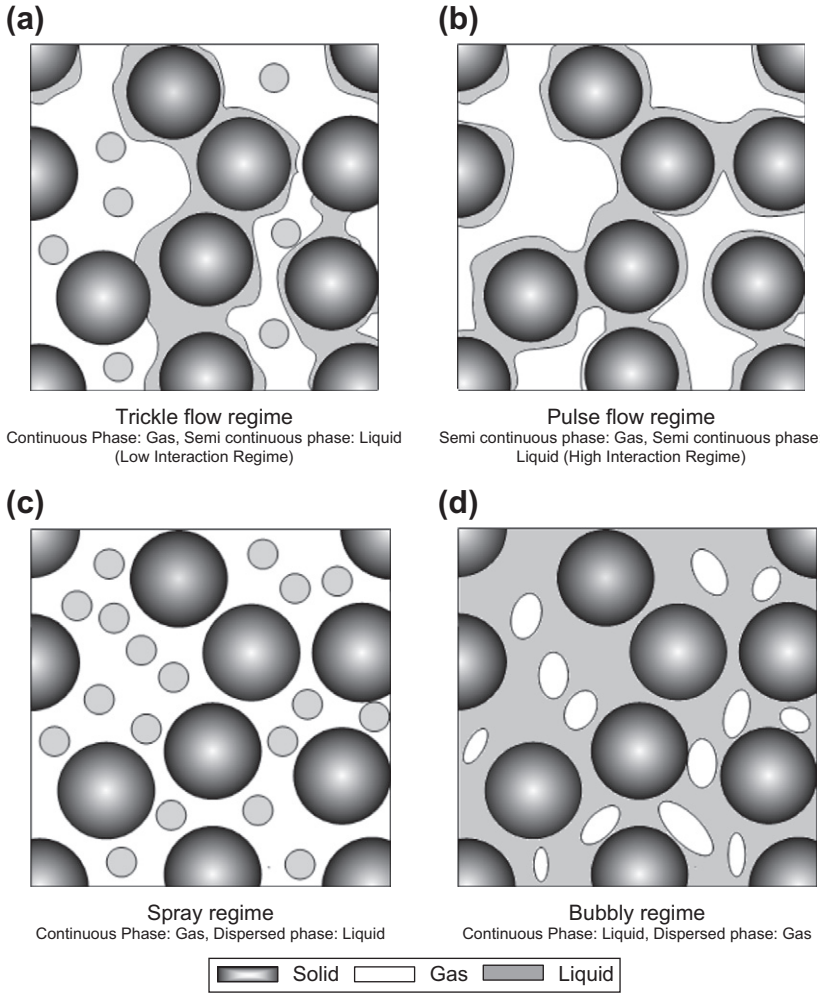

FIGURE 1 Flow regimes in trickle bed reactors (Gunjal et al., 2005).

liquid flow rates, interaction among the phases increases and liquid phase occupies entire flow cross-section. This process leads to the formation of alternate gas–liquid-enriched zones as shown in Fig. 1b and the corresponding regime is classified as pulse flow regime (also referred as high interaction regime). Trickle and pulse flow regimes occur at low-to-moderate flux of gas and liquid flow rates and industrial reactors are commonly operated in these flow regimes. Two other flow regimes (spray and bubbly) may occur at higher gas or liquid flow rates but these are less common in practical conditions. At low gas flow rate and high liquid flow rates, liquid phase occupies entire portion of the bed and becomes continuous phase while gas phase is flowing in the form

of bubbles in the downward direction. This flow regime is known as bubbly flow regime and its schematic is shown in Fig. 1d. On the other hand, at low liquid and high gas flow rates, liquid phase becomes dispersed phase in the form of droplets [see Fig. 1c] and gas phase becomes the continuous phase. This flow regime is known as spray flow regime. Key characteristics of the individual flow regimes are discussed here.

Trickle Flow Regime

Trickle flow regime exists at low liquid and moderate gas flow rates where liquid flows in the form of films or rivulets over the catalyst particles. At low liquid flow rates, inertial forces are weaker compared to the local surface forces and liquid spreading is mainly controlled by capillary pressure. Hence, liquid phase flows in the form of rivulets. However, at higher flow rates, inertial forces become important as compared to the interfacial forces (adhesion, capillary); resulting in film formation over the catalyst surface. The flow regime map reported by Sie and Krishna (1998) is shown in Fig. 2 for air−water system and it is shown that the trickle flow regime exists till 12−15 kg/m^{2}s of liquid flow rates and ~1.25 kg/m^{2}s of gas flow rate. The foaming nature of the liquid phase significantly affects the flow regime boundaries. In such cases, relative importance of surface forces should be considered along with the inertial and viscous forces (see, for example, Gianetto, Baldi, & Specchia, 1970; Morsi, Midoux, & Charpentier, 1978; Talmor, 1977). Trickle flow regime region widens with increase in particle size, decrease in liquid viscosity, and surface tension. Low pressure drop, low gas−liquid throughputs, less catalyst attrition,

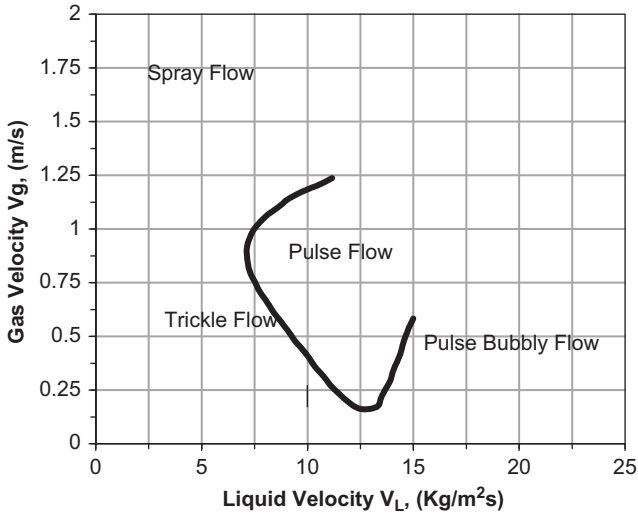

FIGURE 2 Flow regime map (Sie & Krishna, 1998).

and suitability for foaming liquids are some of the advantages of trickle flow operation. Particle wetting may be advantageous or disadvantageous depending upon the reaction type. In trickle flow regime, heat and mass transfer rates are poorer as compared to the other flow regimes. In spite of these issues, many industrial processes operate in this regime to achieve the specific process goals (like higher conversion and productivity).

Pulse Flow Regime

Transition from trickle to pulse flow regime occurs with increase in either gas flow rate or liquid flow rate. The flow regime map reported by Fukushima and Kusaka (1977a) is shown in Fig. 3. This map is in terms of gas and liquid phase Reynolds numbers. In the pulse flow regime, local flow path for gas phase is blocked by liquid pockets/plugs which results in the formation of alternate gas and liquid-enriched zones. In the liquid-enriched zones, complete wetting of particles occurs under this flow regime. Pulse flow regime boundaries are significantly affected by properties of the liquid, i.e., foaming or non-foaming. In the case of non-foaming liquid, gas–liquid-enriched zones are quite distinct and visible. Smaller-sized bubbles get entrapped into the liquid slugs. In the case of a foaming liquid, liquid slugs contain large-sized gas bubbles and the gas fraction in liquid-rich bands is also significant. In such a case, tendency of transition from the pulse flow to bubbly flow regime increases with increase in foaming nature of the liquid (Talmor, 1977). Most of the industrial trickle bed reactors are operated at close to the

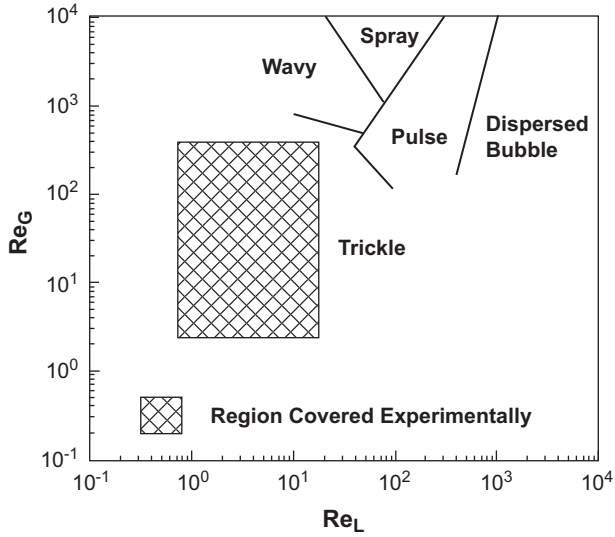

FIGURE 3 Flow regime map (Al-Dahhan & Dudukovic, 1994; Fukushima & Kusaka, 1977b).

boundary of trickle to pulse flow regime (Satterfield, 1975) taking advantages of both operating regimes.

Pulse flow regime has advantages in terms of wetting, effective utilization of catalyst bed, and higher heat and mass transfer rates. However, operating window for pulse flow regime is relatively smaller than other flow regimes such as trickle, spray, and bubbly flow regimes. Large diameter trickle beds are difficult to operate in pulse flow regime. Forced cyclic operation may be an alternative way for such cases in order to get some of the benefits associated with the pulse flow regime.

Spray Flow Regime

At high gas flow rates and low liquid flow rates, liquid film in trickle flow regime is subjected to high shear due to relatively higher slip velocity. Under certain conditions, liquid phase looses its semi-continuous nature and flows in the form of droplets. This regime is called a "spray flow" regime. It is difficult to identify and measure exact boundary between the trickle flow and the spray flow regimes. The flow regime map reported by Saroha and Nigam (1996) is shown in Fig. 4. This map is in terms of key dimensionless numbers and is quite general. Parameters λ and ψ are defined in Fig. 4. G denotes mass flux and subscripts G and L denote gas and liquid phases, respectively. Definitions of other commonly used symbols are listed in *Notations*. This flow regime map may be recommended for identifying prevailing flow regimes in trickle beds.

The spray flow regime typically occurs at $V_G > 1.25\ \text{kg/m}^2\text{s}$ and $V_L < 12\ \text{kg/m}^2\text{s}$. Typical gas phase Reynolds number is larger than 100. The boundary between the trickle and the spray flow regimes is quite sensitive to particle diameter and surface tension as compared to other parameters. Due to higher gas flow rates, gas recycling is required if it is operated under spray flow regime. Low liquid holdup, high gas–liquid mass transfer rates, and low foamability are typical characteristics of this flow regime.

Bubbling Flow Regime

At low gas and high liquid flow rates, liquid occupies entire region of the void space in the packed bed and becomes a continuous phase. Gas flows as a dispersed phase in the form of bubbles. This flow regime is known as bubbling flow. The flow regime map shown in Fig. 4 may also be used for identifying bubbling flow regime. This way an intimate interaction among the phases is possible at the expense of higher pressure drop. Higher liquid holdup leads to back mixing which may not be suitable for some of the reactions. Complete wetting of the bed and high heat and mass transfer rates are some of the advantages of this flow regime and is suitable for cases where liquid phase is a limiting component and reactions are highly exothermic. This flow regime

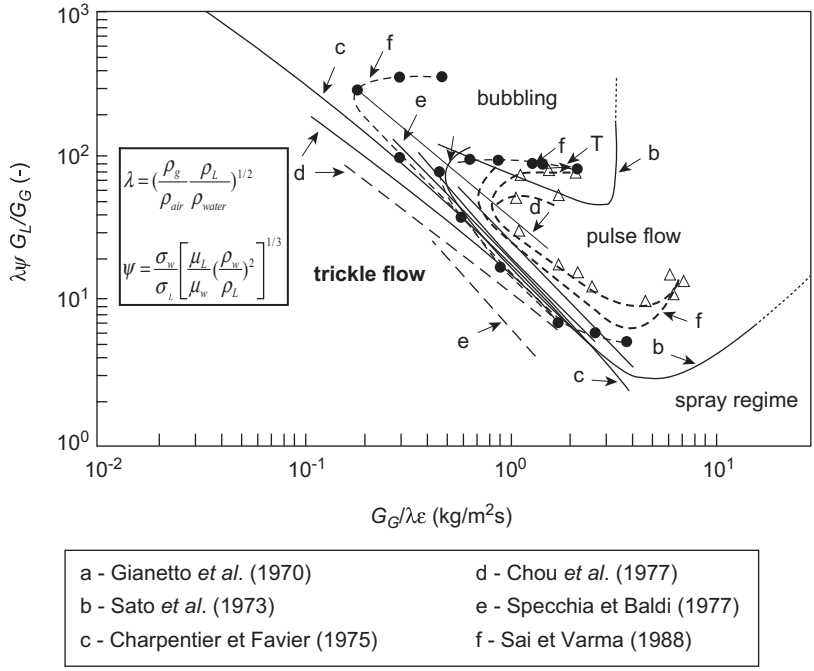

a - Gianetto *et al*. (1970)
b - Sato *et al*. (1973)
c - Charpentier et Favier (1975)
d - Chou *et al*. (1977)
e - Specchia et Baldi (1977)
f - Sai et Varma (1988)

FIGURE 4 Flow regime map (Saroha & Nigam, 1996).

occurs typically at $V_G < 0.75$ kg/m^{2}s and $V_L < 12$ kg/m^{2}s. Flow regime boundaries do not solely depend upon gas–liquid flow rates and are also a function of bed characteristics and fluid properties.

FLOW REGIME TRANSITION

In industrial practice, reactors are often operated close to the flow transition boundary between trickle and pulse flow regimes. This realizes better mass transfer rates, catalyst utilization, and enhances production capacity. It is therefore important to have adequately accurate estimation of trickle–pulse flow regime boundary. Several studies (see, for example, Attou & Ferschneider, 2000; Grosser, Carbonell, & Sundaresan, 1988; Holub, Dudukovic & Ramachandran, 1993; Wammes & Westerterp, 1990) have focused on how and when this transition occurs and its relationship with reactor hardware and operating parameters. Considering the importance of this transition boundary for design and operation of industrial trickle bed reactors, some aspects of transition such as physical picture, methods of detection, and the parameters influencing the transition boundary are briefly discussed here.

As discussed in the earlier section, pulse flow regime occurs with increase in gas or liquid flow rates. For a fixed mass flow rate of the gas, increase in liquid

flow rate leads to increase in local liquid holdup to such an extent that it completely blocks the flow passage for the gas phase. The concept of flow passage blockage is discussed in several studies (Ng, 1986; Sicardi, Gerhard, & Hofmann, 1979). Such a blockage generates disturbances which propagate and grow along the length of the trickle bed. When these disturbances grow to a measurable level, pulse flow regime is observed (Krieg, Helwick, Dillon, & McCready, 1995). In other models, appearance of pulse flow is related to the instability occurring in the liquid film due to the shear exerted by the gas phase (Grosser et al., 1988; Holub et al., 1993). For fixed liquid mass flux, shear exerted by the gas phase on the liquid film drives the excess liquid in the film along the solid surface. Accumulated excess liquid generates blockage to the gas flow passage which eventually leads to pulse formation. Though measurable size of disturbance (pulse) is considered as the inception of pulse flow regime, particle-scale processes suggest that actual inception starts much earlier.

Several experimental methods have been used to detect the transition from trickle to pulse flow regime. Most of the earlier studies were based on visual observations. A change in slope of measured pressure drop or liquid holdup with respect to gas or liquid flow rates may also indicate the transition to the pulse flow regime (Bansal, Wanchoo, & Sharma, 2005; Burghardt et al., 1994; Chou, Worley, & Luss, 1977; Sicardi et al., 1979; see Fig. 5). In recent years, various online sensors and imaging techniques have been used for the identification of flow regime transition, some examples of which are conductivity probes (Tsochatzidis & Karabelas, 1994), micro-electrodes (Latifi et al., 1989), wall pressure fluctuations (Chou et al., 1977; Gunjal, Kashid, Ranade, & Chaudhuri,

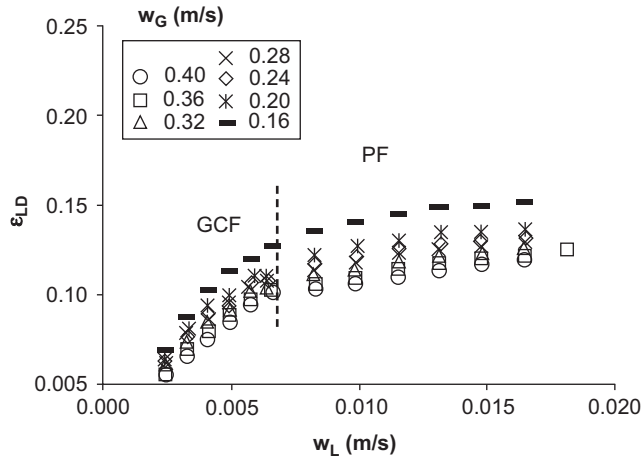

FIGURE 5 Variation of dynamic liquid holdup in trickle and pulse flow regimes (Burghardt, Bartelmus, & Szlemp, 2004). GCF: gas continuous flow; PF: pulse flow; w_G and w_L: gas–liquid superficial velocities, for the air–glycerine (30%) system. P = 1.2 MPa.

2005), computed tomography (CT), magnetic resonance imaging (MRI) (Lutran, Ng, & Delikat, 1991; Sederman et al., 2001), etc.

Experimental studies have identified several key system parameters which influence regime transition. Some of these are particle diameter and its shape factor (d_p and φ), porosity of the bed (ε) and properties of gas−liquid phases (viscosity, density, surface tension, contact angle), column diameter, and operating parameters like pressure, temperature, and gas or liquid flow rates. Inception of pulse flow regime is usually calculated based on critical liquid velocity for transition at the given gas flow rate. The fluid properties can be grouped together in the form of following dimensionless number which can be related to the flow regime transition (Baker, 1954; Bansal et al., 2005):

$$\lambda = \left[\left(\frac{\rho_G}{\rho_{air}}\right)\left(\frac{\rho_L}{\rho_W}\right)\right]^{1/2} \text{ and } \xi = \left(\frac{\sigma_W}{\sigma_L}\right)^{3.5}\left(\frac{\mu_L}{\mu_W}\right)^{0.5}\left(\frac{\rho_W}{\rho_L}\right)^{1/3} \quad (1)$$

The subscript W denotes the property of "water." Relevant correlations which may be used for estimating regime transition are summarized in Table 1. Bansal et al. (2005) have accounted for the influence of particle diameter and non-Newtonian behavior of fluids in their correlations.

Few attempts have been made to develop models and correlations based on physical understanding of the transition. Wammes & Westerterp (1990) have derived a correlation based on a criterion that assumes transition occurring at some critical dynamic holdup and it is related to the operating parameters as follows:

$$j_G^{0.26} = \frac{C}{\beta_{t,tr}\rho_G^{0.04}} \quad (2)$$

where, $C = 0.27$ for water−N_2 and 0.32 for 40% ethylene glycol−N_2. j_G is the gas superficial velocity in m/s and $\beta_{t,tr}$ denotes the total liquid saturation (ratio of static + dynamic liquid holdup to void volume fraction).

Another criterion is proposed by Holub et al. (1993) based on loss of the stability of laminar liquid film during the inception of the pulse flow regime. A phenomenological criterion is developed on the basis that instability of waves on the surface of the liquid film appears due to high shear exerted by the gas phase. For this purpose, Kapitza's criterion is used for calculating occurrence of surface waves and it is related to the operating parameters in the following manner (Holub et al., 1993):

$$\frac{2.90 Re_L E_1^{5/11}}{\psi_L^{0.17} Ga_L^{0.41} Ka^{1/11}} \leq 1, \quad \psi_L^{0.17} = \frac{1}{\rho_L g}\frac{dP}{dZ} + 1$$
$$2.8 < Ga_L < 6.3, \quad 1 < \psi_L < 55 \quad (3)$$

TABLE 1 Empirical Correlations for Estimation of Trickle to Pulse Flow Regime Transition (λ and ξ are defined in Eq. (1))

Author	Correlations
Larachi, Laurent, Wild, and Midoux (1993) $\Phi = \frac{1}{4.76 + 0.5\frac{\rho_G}{\rho_a}}$ and $\psi = \frac{\sigma_W}{\sigma_L}\left(\frac{\mu_L}{\mu_W}\right)^{1/3}\left(\frac{\rho_W}{\rho_L}\right)^{2/3}$	$\frac{L_t\lambda\psi\Phi}{G} = \left(\frac{G}{\lambda}\right)^{-1.25}$
Wang, Mao, and Chen (1994)	$L_t\lambda\psi = 4.864\left(\frac{G}{\lambda}\right)^{-0.337}, \quad \frac{G}{\lambda\varepsilon} = 1$
Dudukovic and Mills (1986)	$L_t = \min\left[\frac{10^3 G}{\lambda\psi}5.43\frac{\varepsilon}{\psi}\left(\frac{\lambda\varepsilon}{G}\right)^{0.22}\right]$
Bansal et al. (2005) where, $S_1 = \frac{a_s d_p}{\varepsilon}$ and $S_2 = \left(\frac{1}{d_{ps}}\right)\frac{1}{\phi}$ $\frac{L_t\lambda\psi\varphi}{G} = \left(\frac{G}{\lambda}\right)^{-1.25}$ $We = \lambda_{eff}\cdot\dot{\gamma}_W$ $\dot{\gamma}_W = \frac{3n+1}{4n}\frac{8V_0}{\varepsilon D_e}\frac{k_i}{2}, \quad \lambda_{eff} = \frac{N_1}{2\dot{\gamma}\tau}$	For Newtonian liquid phase $\left(\frac{L_i}{G}\right)\lambda\xi\left(\frac{S_2}{S_1^2}\right)^{1/4} = 5.73\left(\frac{G}{\lambda\varepsilon}\right)^{-4/3}$ For non-Newtonian (visco-inelastic) liquid phase $\left(\frac{L_{t,vi}}{G}\right)\lambda\xi'\left(\frac{S_2}{S_1^2}\right)^{1/4} = 5.73\left(\frac{G}{\lambda\varepsilon}\right)^{-4/3}$ For non-Newtonian (visco-elastic) liquid phase $L_{t,ve} = L_{t,ve}(1 + \sqrt{2}We^{-2})$

where the Galileo number, $Ga_L = d_p^3\rho_L^2 g\varepsilon^3/\mu_L^2(1-\varepsilon)^3$ and Kapitza number, $Ka = \sigma_L^3\rho_L/\mu_L^4 g$. This semi-empirical model requires knowledge of liquid phase pressure drop and Ergun constant E_1 and is suitable for estimation of the flow regime boundary for the reactors operated at or near atmospheric pressure.

Grosser et al. (1988) have used linear stability analysis of one-dimensional model (Eqs.(4) and (5)) for estimating the regime transition boundary.

$$\frac{\partial\varepsilon_i}{\partial t} + \nabla(\varepsilon_i u_i) = 0 \tag{4}$$

$$\rho_i\varepsilon_i\left(\frac{\partial u_i}{\partial t} + u_i\cdot\nabla u_i\right) = -\varepsilon_i\nabla P_i + \varepsilon_i\rho_i g + F_i \tag{5}$$

where, u is interstitial velocity of ith phase (gas or liquid).

Pressure difference in the gas and liquid phases (capillary pressure) is correlated using the Leverett's function (Scheidegger, 1974) as:

$$P_G - P_L = \left(\frac{\varepsilon}{k}\right)^{1/2} \sigma J(\varepsilon_L), \quad \text{where } J(\varepsilon_L) = 0.48 + 0.36 \ln\left(\frac{\varepsilon - \varepsilon_L}{\varepsilon_L}\right). \quad (6)$$

where, P is pressure, ε is porosity, and k is permeability of fluid. For the interphase drag force terms (F_i), the semi-empirical form of expressions provided by Saez and Carbonell (1985) were used:

$$F_G = -\left[\frac{A\mu_G(1-\varepsilon)^2\varepsilon^{1.8}}{d_p^2\varepsilon_G^{2.8}} + \frac{B\rho_G(1-\varepsilon)\varepsilon^{1.8}|u_G|}{d_p\varepsilon_G^{1.8}}\right] u_G \quad (7)$$

$$F_L = -\left\{\frac{\varepsilon - \varepsilon_s}{\varepsilon_l - \varepsilon_s}\right\}^{2.9} \left[\frac{A\mu_L(1-\varepsilon)^2\varepsilon^2}{d_p^2\varepsilon^3} + \frac{B\rho_L(1-\varepsilon)\varepsilon^3|u_L|}{d_p\varepsilon^3}\right] u_L \quad (8)$$

where, ε_{LS} is static liquid holdup, $\varepsilon_{LS} = (20 + 0.9E)^{-1}$, and $E = \rho_L g d_P^2 \varepsilon^2 / \sigma(1-\varepsilon)^2$.

Though this approach uses fundamental equations of hydrodynamics, some terms appearing in the equations (capillary pressure, relative permeability, static liquid holdup, interphase drag, etc.) are based on empirical correlations. Attou and Ferschneider (2000) have developed models to reduce the empiricism associated with these parameters. Capillary pressure is expressed by them in terms of gas holdup and particle diameter as:

$$P_G - P_L = 2\sigma\left(\frac{1-\varepsilon}{1-\varepsilon_G}\right)^{1/3}\left(\frac{1}{d_p} - \frac{1}{d_{min}}\right), \quad \text{where } d_{min} = \left(\frac{\sqrt{3}}{\pi} - \frac{1}{2}\right)^{1/2} d_p \quad (9)$$

The formulation of interphase forces is based on Ergun's equation in which liquid phase is considered as an additional phase to the gas flow in the packed bed and their expressions take the following forms (Attou & Ferschneider, 2000):

Gas–liquid momentum exchange term:

$$F_{GL} = \varepsilon_G\left(\frac{E_1\mu_G(1-\varepsilon_G)^2}{d_p^2\varepsilon_G^2}\left[\frac{\varepsilon_S}{(1-\varepsilon_G)}\right]^{0.667} + \frac{E_2\rho_G(U_G - U_L)(1-\varepsilon_G)}{d_p\varepsilon_G}\left[\frac{\varepsilon_S}{(1-\varepsilon_G)}\right]^{0.333}\right) \quad (10)$$

Gas−solid momentum exchange term:

$$F_{GS} = \varepsilon_G \left(\frac{E_1 \mu_G (1-\varepsilon_G)^2}{d_p^2 \varepsilon_G^2} \left[\frac{\varepsilon_S}{(1-\varepsilon_G)} \right]^{0.667} + \frac{E_2 \rho_G U_G (1-\varepsilon_G)}{d_p \varepsilon_G} \left[\frac{\varepsilon_S}{(1-\varepsilon_G)} \right]^{0.333} \right) \quad (11)$$

Liquid−solid momentum exchange term:

$$F_{LS} = \varepsilon_L \left(\frac{E_1 \mu_L \varepsilon_S^2}{d_p^2 \varepsilon_L^2} + \frac{E_2 \rho_L U_G \varepsilon_S}{d_p \varepsilon_L} \right) \quad (12)$$

Linear stability analysis of one-dimensional flow equations and their subcomponents (Eqs. (10)−(12)) provides prediction of the flow regime transition boundaries more accurately than empirical correlations derived from the experimental data (Attou & Ferschneider, 2000). Influence of various system parameters (bed geometry, operating parameters, and fluid properties) on the transition of regimes is briefly discussed in the following.

In smaller diameter trickle beds, inception of pulse flow regime is observed earlier than the larger diameter columns. Reactor diameter plays a significant role in the formation of blockage in the form of liquid-rich zone. It is usually difficult to operate larger diameter trickle bed reactors in a pulse flow regime. For larger diameter particles, capillary forces are less dominant than gravitational forces. Therefore the liquid holdup in the bed is substantially lower for the larger-sized particles. The transition to pulse flow therefore gets delayed for larger-sized particles (Gunjal et al., 2005). Similar phenomenon is observed in higher porosity beds (Chou et al., 1977; Sai & Varma, 1988).

Influence of gas−liquid throughput on the trickle to pulse flow regime boundary is shown in Fig. 6. At higher gas or liquid throughputs, inertial forces attenuate waves on the liquid film which are responsible for destabilization of the trickle flow pattern. Therefore, for higher gas throughputs, transition to pulse flow regime occurs at smaller liquid flow rates and vice versa (Attou & Ferschneider, 2000; Grosser et al., 1988; Ng, 1986).

Gas and liquid phase properties also have significant effect on transition boundary. Effect of capillary force can be significantly reduced by decrease in surface tension of the liquid. Experiments carried out by Charpentier and Favier (1975), Chou et al. (1977), and Wammes & Westerterp (1991) demonstrated such effects on flow regime transition boundary where water and cyclohexane were used as the liquid phases. Cyclohexane with lower surface tension (3 times lower than water) shows early inception of the pulse flow regime (see Fig. 7).

Influence of gas phase viscosity and liquid phase density on transition boundary is rather small as compared to the liquid phase viscosity and gas

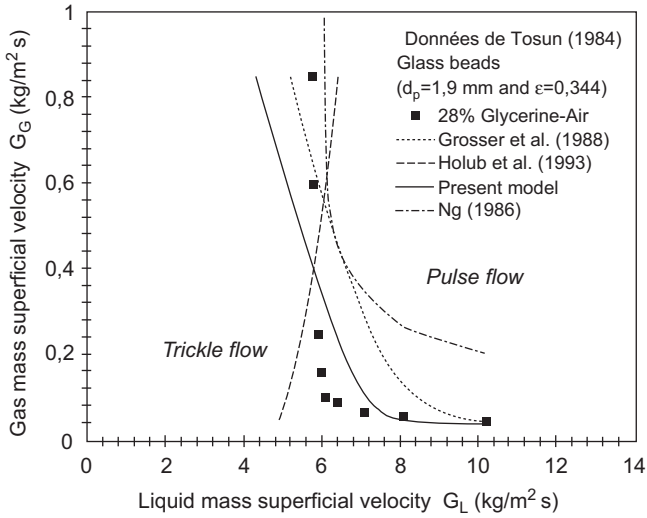

FIGURE 6 Effect of gas and liquid throughputs on trickle to pulse flow regime transition boundaries (Attou & Ferschneider, 2000).

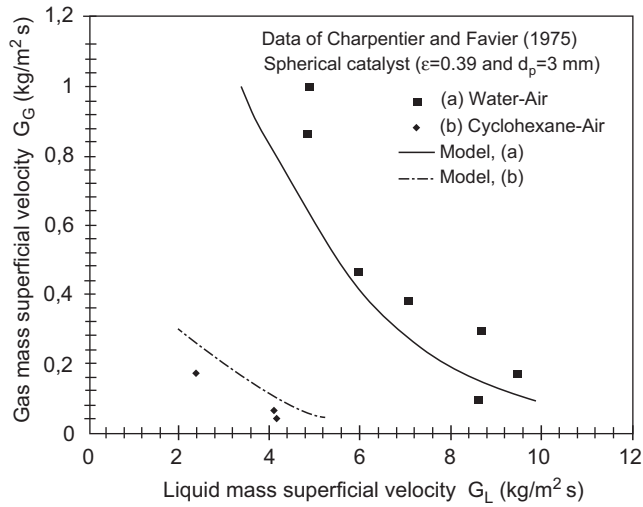

FIGURE 7 Effect of surface tension on trickle to pulse flow regime transition boundaries (Attou & Ferschneider, 2000).

phase density. Higher liquid phase viscosity leads to increase in liquid holdup, and therefore earlier inception of the pulse flow regime. Available experimental data confirm these trends (Morsi, Midoux, Laurent, & Charpentier, 1982; Sai & Varma 1988; Wammes & Westerterp, 1991). Most of the industrial trickle bed reactors are operated at high pressures. It is therefore important to understand

the influence of operating pressure (or gas density) on the regime boundary. Al-Dahhan and Dudukovic (1994) have shown that effect of operating pressure is negligible as long as gas density is below 2.3 kg/m^3. However, effect of operating pressure is significant when gas density exceeds 2.3 kg/m^3. Attou and Ferschneider (2000) have attributed effect of increase in gas density to decrease in inertial forces; therefore transition boundary occurs at higher gas and liquid velocities. Experimental data of Wammes & Westerterp (1991) demonstrated the effect of operating pressure on transition boundary (see Fig. 8).

Despite years of experimental and modeling efforts, estimation of trickle to pulse flow regime transition is still not very accurate. Earlier models (Ng, 1986; Sicardi & Hofmann, 1980) assumed that inception of pulse flow occurs at pore-scale level, while recent models (Attou & Ferschneider, 2000; Grosser et al., 1988; Holub, Dudukovic, & Ramachandran, 1992) considered it as a bed-scale (macro-scale) phenomenon. Though macroscopic models have shown relatively better agreement with the experimental data, experimental data also indicate the importance of pore-scale processes in the inception of regime transition. Therefore, understanding physical phenomenon associated with inception of pulse flow is still a challenge and further efforts based on multi-scale modeling approach may lead to improvements in estimation of regime transition. In the mean time, equations and regime maps included here may be used for estimating the regimes and transition boundaries. *Estimation of key hydrodynamic parameters* is discussed in the following section.

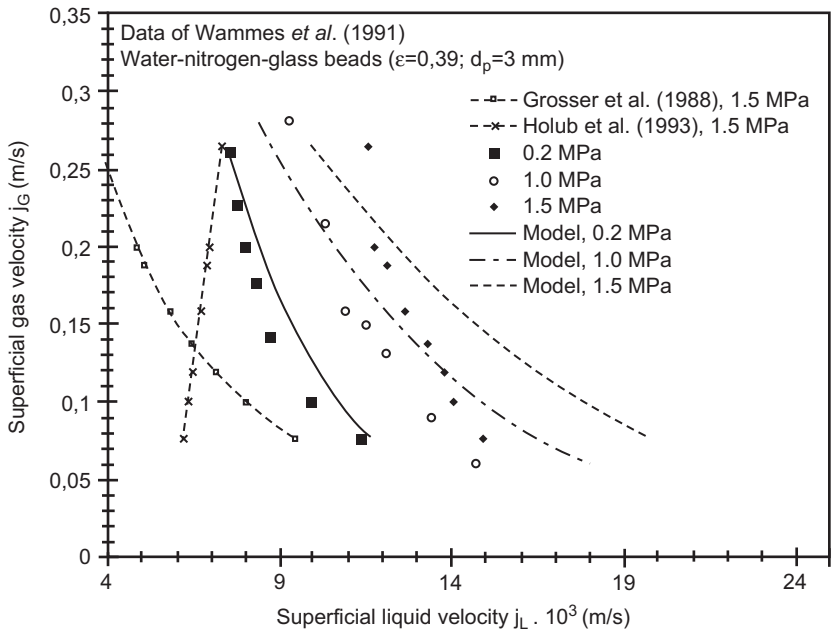

FIGURE 8 Effect of operating pressure on trickle to pulse flow regime transition boundaries.

ESTIMATION OF KEY HYDRODYNAMIC PARAMETERS

Pressure Drop

Pressure drop in trickle bed reactors is one of the most important design parameters. It is one of the key interaction indices for the overall system and therefore is often used as correlating parameter for prediction of other design parameters such as gas–liquid, liquid–solid mass transfer coefficient, wetting efficiency, and heat transfer coefficient. Two-phase pressure drop along the length of the bed is a function of (1) the reactor hardware such as column diameter, particle size and shape, and internals; (2) operating parameters such as gas–liquid flow rates (flow regime); and (3) fluid properties like density and viscosity of flowing fluid, surface tension, and surface characteristics. Operating pressure and temperature indirectly affect the pressure drop through fluid properties.

Reactor column diameter (D) has relatively lower influence on pressure drop as compared to the particle diameter (d_p). This influence is more significant for low D/d_p ratio ($D/d_p < 0.23$). For high D/d_p ratio, variation of pressure drop with column diameter is almost negligible. For low D/d_p ratio, variation of porosity near the wall plays an important role. Due to high porosity near wall, fluid bypassing occurs, resulting in a lower pressure drop. In large diameter

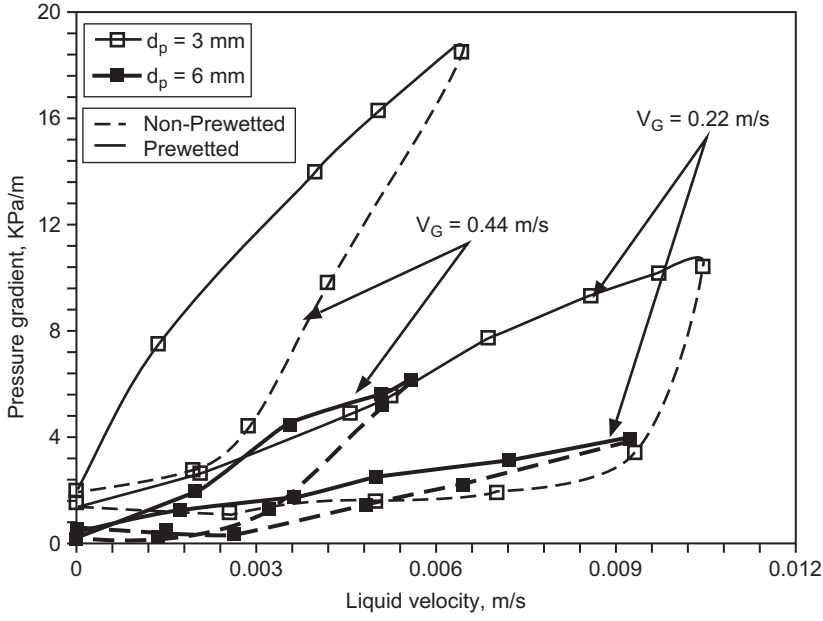

FIGURE 9 Variation of pressure drop at different bed and particle diameters for prewetted and non-prewetted conditions (Gunjal et al., 2005; $D = 11.4$ cm).

columns, uniform distribution of liquid phase is rather difficult. Liquid maldistribution across the bed cross-section may lead to lower interaction among the phases and therefore lower pressure drop. Trickle bed reactors are often operated at low liquid flow rates which cause incomplete wetting of particles. Pressure drop for incompletely wetted particles is often less than completely wetted particles. It is highest for uniformly distributed liquid and completely wetted particles. However, at lower liquid flow rates, measured pressure drop values often show large variation due to non-uniform liquid spreading and wetting.

Particle size and shape also affect the bed pressure drop considerably. Pressure drop is less sensitive to shape factor as compared to the porosity of the bed. Denser beds (lower porosity) lead to higher pressure drop. Pressure drop increases with decrease in size of the particle. Fluid has to follow more tortuous path in the bed with smaller-sized particles. The commercial trickle beds therefore generally use particles in the range of 1 mm to 3 mm to strike appropriate balance of pressure drop and catalyst utilization. A sample of experimental results indicating pressure drop in trickle beds as a function of liquid velocity for two different particle sizes is shown in Fig. 9.

Typical variation of pressure drop with liquid flow rate at a constant gas flow rate is shown in Fig. 10. Pressure drop variation with liquid flow rate shows hysteresis behavior in trickle flow regime (see Figs. 9 and 10) which results due to different bed wetting characteristics while increasing and decreasing the flow rates. Pressure drop for non-prewetted bed is represented by the lower curve due to low interaction between gas and liquid phases. Difference between upper and

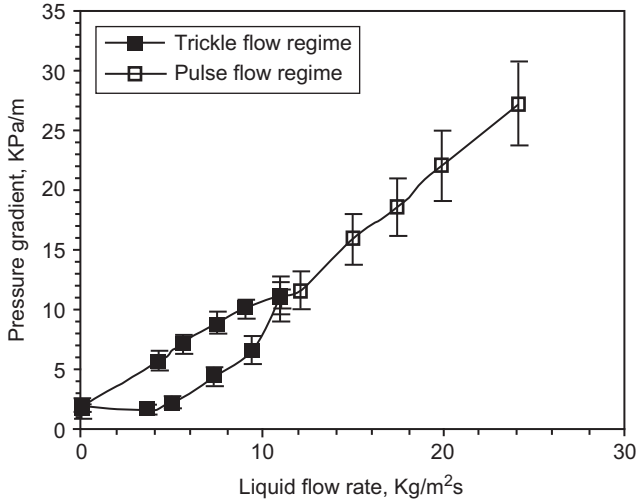

FIGURE 10 Pressure drop in trickle bed reactors (from Gunjal et al., 2005; $D = 0.141$ m, $d_p = 0.003$ m, $V_G = 0.22$ m/s).

lower branches indicates that capillary pressure is significant for non-prewetted bed which restricts the spreading of liquid over solid surface. This effect is negligible for trickle flow operation with prewetted bed or in pulse flow regime.

Reactor hardware (reactor diameter, particle size and shape, etc.) and gas−liquid throughputs have significant effect on the pressure drop. Hence most of the correlations were expressed in terms of Reynolds number of gas and liquid phases. For example, correlation of Kan and Greenfield (1979) for pressure drop is

$$\frac{\left(\frac{\Delta P}{L}\right)_{\mathrm{LG}}}{\left(\frac{\Delta P}{L}\right)_{\mathrm{G}}} = 0.024 d_{\mathrm{p}} \mu_{\mathrm{L}} \left(\frac{\varepsilon_{\mathrm{B}}}{1-\varepsilon_{\mathrm{B}}}\right)^{3} \left(\frac{Re_{\mathrm{G}} We_{\mathrm{G}}}{Re_{\mathrm{L}}}\right)^{-1/3} \tag{13}$$

where ε_{B} is the bed porosity, Re, the Reynolds number based on particle $Re_{\alpha} = (\rho_{\alpha} U_{\alpha} d_{\mathrm{p}}/\mu_{\alpha})$, and We, the Weber number defined as $We_{\mathrm{G}} = (\rho_{\mathrm{G}} U_{\mathrm{G}}^2 d_{\mathrm{p}}/\sigma_{\mathrm{G}})$. The subscripts L and G denote liquid and gas phases, respectively. The above correlation is valid for trickle as well as pulse flow regimes operated at atmospheric pressure and temperature conditions. Several correlations are available for wider range of properties of gas, liquid, and solids (see, for example, those listed in Saez & Carbonell, 1985; Sai & Varma, 1987). Note that these correlations require knowledge of single-phase pressure drop which itself is a function of bed properties. Another class of correlations uses modified Lockhart−Martinelli number instead of single-phase pressure drop. The modified Lockhart−Martinelli number is defined as:

$$X_{\mathrm{L}} = \frac{1}{X_{\mathrm{G}}} = \frac{U_{\mathrm{L}}}{U_{\mathrm{G}}} \left(\sqrt{\frac{\rho_{\mathrm{L}}}{\rho_{\mathrm{G}}}}\right) \tag{14}$$

Using this number, Ellman, Midoux, Laurent, and Charpentier (1988) have proposed the following correlation which is applicable for low as well as high interaction flow regimes for operating pressure in the range of 0.1−10 MPa:

$$\frac{\Delta P}{L} = \frac{2\rho_{\mathrm{G}} U_{\mathrm{G}}^2 [A(X_{\mathrm{G}}\xi_1)^j + B(X_{\mathrm{G}}\xi_1)^k]}{d_{\mathrm{p}}},$$

$$\text{for low interaction regime,} \quad \xi_1 = \frac{Re_{\mathrm{L}}^2}{(0.001 + Re_{\mathrm{L}}^{1.5})},\ A = 200;\ B = 85;$$

$$j = -1.2,\ k = -0.5,$$

$$\text{for high interaction regime,} \quad \xi_1 = \frac{Re_{\mathrm{L}}^{0.25} We_{\mathrm{L}}^{0.2}}{(1 + 3.17 Re_{\mathrm{L}}^{1.65} We_{\mathrm{L}}^{1.2})^{0.1}},\ A = 6.96;$$

$$B = 53.27;\ j = -2;\ k = -1.5. \tag{15}$$

Ergun's equation is widely used for calculating single-phase pressure drop in packed beds. This has been extended for the two-phase flow through packed beds in many studies. For example, the correlation proposed by Wammes & Westerterp (1991) is given in Eq. (16) and that by Benkrid, Rode, and Midoux (1997) in Eq. (17).

$$\frac{\Delta P}{L}\frac{d_p}{(1/2)\rho_G U_G^2} = 155\frac{(1-\varepsilon)}{\varepsilon_G}\left(\frac{\rho_G U_G d_p \varepsilon}{\mu_G(1-\varepsilon)}\right)^{-0.37} \tag{16}$$

$$\frac{\Delta P}{L} = \frac{1}{\varepsilon^3}\left(\frac{\frac{U_G}{U_L}+1}{A\frac{U_G}{U_L}+1}\right)\left(\frac{E_1}{36}\left(\frac{6(1-\varepsilon)}{d_p}+\frac{4}{D}\right)^2 \mu_L U_L + \frac{E_2}{6}\left(\frac{6(1-\varepsilon)}{d_p}+\frac{4}{D}\right)\rho_L U_L^2\right) \tag{17}$$

where E_1 and E_2 are parameters of Ergun equation and A is a constant which is suggested as 0.49 for the above equation (Benkrid et al., 1997).

Pressure drop in pulse flow regime exhibits significant fluctuations which can be reported in two ways: (1) Pressure drop averaged over pulse and base regions as shown in Fig. 10. The error bars (indicating fluctuations) on pressure drop data increase as pulsing increases (see Fig. 10). (2) Alternatively, separate values of pressure drop are measured for the pulse and the base regions (regions between the pulse regions) as shown in Fig. 11.

Two-phase pressure drop is naturally a function of fluid properties. Gas phase viscosity has negligible influence compared to the liquid phase

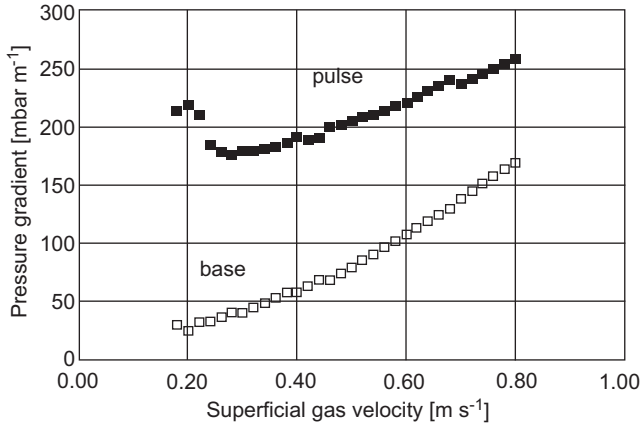

FIGURE 11 Pressure drop in pulse and base regions (Boelhouwer, Piepers, & Drinkenburg, 2002; $d_p = 6$ mm, $D = 0.11$ m, $\varepsilon = 0.38$).

viscosity. Higher viscosity of liquid leads to higher values of pressure drop. Foaming liquids are prone to produce higher gas–liquid interfacial area and therefore higher energy loss/pressure drop is associated with such systems (Larachi, Laurent, Midoux, & Wild, 1991; Midoux, Favier, & Charpentier, 1976). The following correlation proposed by Larachi et al. (1991) is valid for foaming and non-foaming liquids for 0.2–8.1 MPa operating pressure.

$$\frac{\Delta P}{L} = \frac{2G_G^2}{d_h \rho_G (X_G (Re_L We_L)^{1/4})^{3/2}} \left[31.3 + \frac{17.3}{\sqrt{X_G (Re_L We_L)^{1/4}}} \right] \tag{18}$$

where, d_h is hydraulic diameter ($d_h = d_p \sqrt[3]{16\varepsilon^3/9\pi(1-\varepsilon)^2}$) and X_G is the modified Lockhart–Martinelli number defined in Eq. (14).

Influence of operating pressure on pressure drop across a trickle bed is shown in Fig. 12. Pressure drop at high pressure conditions is similar to that operated with a gas of high molecular weight under lower pressure (provided that density of gas under operating conditions is similar). Figure 12 illustrates such an effect where pressure drop for the bed operated at 0.34 MPa with nitrogen gas is comparable with the bed operated at high pressure (2.13 MPa) with helium gas. Most of the previous correlations were developed based on the experimental data collected at atmospheric conditions and may not be useful for reactors operated at high pressure. The correlations proposed by Holub et al. (1992) (Eq. (19)), Larachi et al. (1991) (Eq. (18)), and Wammes & Westerterp (1991) (Eq. (16)) are applicable over a range of operating pressures (0.1–10 MPa).

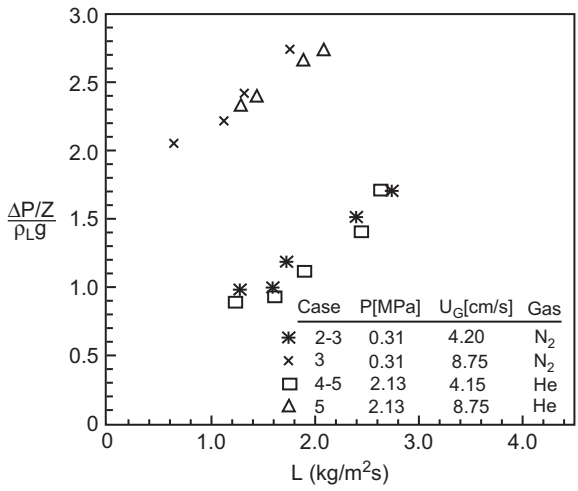

FIGURE 12 Effect of operating pressure on pressure drop in trickle bed reactors (Al-Dahhan & Dudukovic, 1994). System: hexane, nitrogen, and helium, with $D =$ 0.022 m; $d_p = 1.14$ mm glass beads.

Correlation proposed by Holub et al. (1992) is as follows:

$$\psi_L = \frac{\Delta P}{\rho_L g Z} + 1 = \left(\frac{\varepsilon}{\varepsilon_L}\right)^3 \left[\frac{E_1 Re_L}{Ga_L} + \frac{E_2 Re_L^2}{Ga_L}\right],$$

$$\psi_G = \frac{\Delta P}{\rho_G g Z} + 1 = \left(\frac{\varepsilon}{\varepsilon - \varepsilon_L}\right)^3 \left[\frac{E_1 Re_G}{Ga_G} + \frac{E_2 Re_G^2}{Ga_G}\right],$$

$$\psi_L = 1 + \frac{\rho_G}{\rho_L}[\psi_G - 1]. \tag{19}$$

Prediction of pressure drop in trickle bed reactors is an important design parameter. It is sensitive to the particle packing characteristics as well as to the properties of the flowing fluids. Many earlier pressure drop correlations for gas–liquid flow through packed beds were based on the data obtained with packing like Raschig rings and hollow cylinders. These correlations often under-predict the pressure drop for particles with spherical or trilobe shapes. It is therefore important to select appropriate pressure drop correlation based on prevailing flow regime, reactor scale, particle sizes and shapes, properties of the fluid, and operating pressure and temperature.

Liquid Holdup

Liquid holdup in trickle bed reactor is expressed in two ways : (i) total liquid holdup (ε_L) defined as volume of liquid per unit bed volume and (ii) liquid saturation (β_L) defined as volume of liquid per unit void volume instead of unit bed volume. Liquid holdup is composed of two parts: dynamic liquid holdup (ε_{Ld}) and static liquid holdup (ε_{Ls}). Static liquid holdup is the volume of liquid per unit volume of bed which remains in the bed after draining the bed. Many other design parameters of trickle bed reactors, like wetting efficiency and heat and mass transfer coefficients, are dependent on liquid holdup. The prevailing liquid holdup in the bed also controls the liquid phase residence time and therefore conversion of the reactants. It is therefore essential to understand how liquid holdup varies with (1) reactor hardware such as column diameter, particle size and shape, and internals, (2) operating parameters such as gas and liquid flow rates, and (3) physico-chemical properties of fluids. Available information on this is briefly discussed in the following.

Liquid holdup is sensitive to variation in bed diameter at low D/d_p ratio and increases with the bed diameter for a given particle size (Gunjal et al., 2005). For smaller column diameters, flow bypassing results in lower pressure drop which causes low gas–liquid interaction. Therefore, liquid holdup is higher for the lower diameter columns where flow bypassing occurs. However, for larger diameter columns, liquid holdup is less sensitive to the column diameter due to negligible wall effects. Liquid holdup is considerably sensitive to particle

diameter than bed diameter. Specific area of solid particles is higher for the smaller-sized particles (Gunjal et al., 2005; Rao, Ananth, & Varma, 1983); leading to higher liquid phase retention and holdup. Following correlations proposed by Burghardt, Bartelmus, Jaroszynski, and Kolodziej (1995) (Eq. (22)) and Specchia and Baldi (1977) (Eqs. (20) and (21)) demonstrate the dependency of dynamic liquid holdup to the particle diameter and interfacial area in low and high interaction regimes. These correlations are valid for a bed operated at atmospheric conditions.

For low interaction regime:

$$\beta_d = 3.86 Re_L^{0.545} (Ga^*)^{-0.42} \left(\frac{a_s d_p}{\varepsilon}\right)^{0.65}, \quad 3 < Re_L < 470 \tag{20}$$

where β_d is dynamic liquid holdup, a_s is specific surface area of solid, and $Ga^* = d_p^3 \rho_L (\rho_L g + \Delta P/\Delta Z/\mu_L^2)$.

For high interaction regime:

$$\beta_d = 0.125 \left(\frac{Z}{\psi^{1.1}}\right)^{-0.312} \left(\frac{a_s d_p}{\varepsilon}\right)^{0.65}, \quad 1 < Z/\psi^{1.1} < 500$$
$$\psi = (\delta_W/\delta_L)\left[\left(\mu_L/\mu_W\right)(\rho_W/\rho_L)^2\right]^{0.33} \tag{21}$$

where δ is pressure drop per unit length for a single-phase flow.

$$\beta_d = 1.125(Re_G + 2.28)^{-0.1} (Ga'_L)^{-0.5} \times \left(\frac{a_s d_p}{\varepsilon}\right)^{0.3} \tan h\left(48.9 (Ga'_L)^{-1.16} Re_L^{0.41}\right),$$
$$\text{for } 2 < Re_L < 62, 0 < Re_G < 103, 51 < Ga'_L < 113 \tag{22}$$

where, $Ga' = d_p/(\mu_L^2/(g\rho_L^2))^{1/3}$.

Similar to pressure drop, liquid holdup also exhibits hysteresis behavior with variation in gas and liquid flow rates. The magnitude of hysteresis depends on the extent of prewetting of the bed. Extent of hysteresis is highest when the bed is at fully dry conditions.

Gas and liquid phase throughputs have significant effect on the liquid holdup. In the case of low interaction regime (both gas and liquid flow rates are lower), liquid holdup is insensitive to the gas flow rate. At moderate and high gas and liquid flow rates, liquid holdup decreases with increase in gas flow rate. Contrary to this trend, the liquid holdup increases with liquid flow rate because of displacement of gas phase by the liquid. In a trickle flow regime, this displacement occurs till liquid occupies maximum possible region. Therefore, rate of increment in holdup with liquid flow rate is higher compared to the pulse flow regime (see Fig. 13). In pulse flow regime, marginal increment in holdup

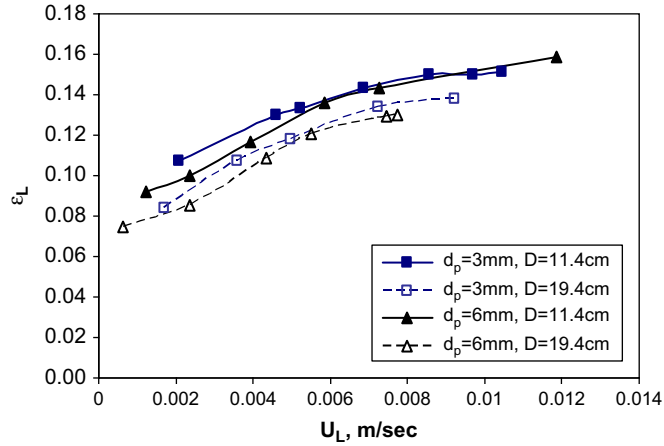

FIGURE 13 Effect of gas and liquid flow rates on dynamic liquid holdup (Burghardt et al., 2004).

values with liquid flow rate indicates that a scope for gas phase replacement is limited compared to the trickle flow regime. Thus, the decrease in liquid holdup is attributed to increase in shear between gas and liquid phases. In the case of pulsing flow, overall liquid holdup is composed of holdup in the base region and pulse flow region. Such representation of liquid holdup for pulsing regime is illustrated in Fig. 14. In pulse flow regime, both pulse and base holdups are comparatively less sensitive to the liquid flow rate than gas flow rates. Following correlations are useful for the prediction of liquid holdup in different flow regimes for reactors operated at atmospheric conditions. Simple form of

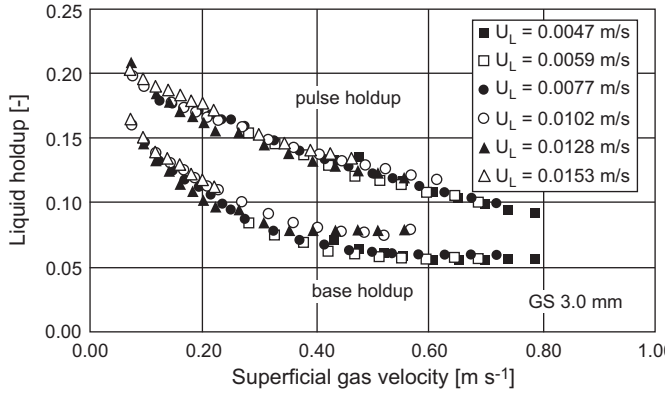

FIGURE 14 Effect of gas and liquid flow rates on dynamic liquid holdup (Boelhouwer et al., 2002). System: $D = 0.05$ m; $d_p = 3$ mm sphere, $\varepsilon = 0.4$.

correlation proposed by Wammes & Westerterp (1991) is based on Reynolds and Galileo number as follows:

$$\begin{aligned}\beta_{nc} &= 16.3 Re_L^c Ga_L^d \\ c &= 0.36 \text{ and } d = -0.39 \quad \text{for } Re < 11 \\ c &= 0.55 \text{ and } d = -0.42 \quad \text{for } Re > 15\end{aligned} \tag{23}$$

where, β_{nc} is non-capillary liquid saturation.

Similar to the pressure drop, liquid holdup can also be related with the Lockhart–Martinelli number (X) as shown in the correlation proposed by Morsi et al. (1982). This correlation derived from the experimental data collected using air and various liquids (cyclohexane, kerosene, and polyethyleneglycol) for D/d_p=20.83 is given here:

$$\begin{aligned}\beta_t &= 0.66X^{0.81}/(1+0.66X^{0.81}), \quad 0.1 < X < 80 \\ \beta_t &= 0.92X^{0.3}/(1+0.92X^{0.3}), \quad 0.05 < X < 100 \\ \beta_t &= 4.83X^{0.58}/(1+4.83X^{0.58})\end{aligned} \tag{24}$$

where β_t is the total liquid saturation and X is the Lockhart–Martinelli number ($X = (dP/dz)_L/(dP/dz)_G$). Rao et al. (1983) have extended this approach to include the effect of various shapes of the particles (spherical, cylindrical, and Raschig ring) for the low and high interaction regimes. They arrived at the following generalized form of correlation:

$$\begin{aligned}\beta_t &= cX^b a_s^{1/3} \\ c &= 0.4,\ b = 0.23 \quad \text{for trickle flow regime} \\ c &= 0.4,\ b = 0.27 \quad \text{for pulse flow regime} \\ c &= 0.38,\ b = 0.2 \quad \text{for bubbly flow regime}\end{aligned} \tag{25}$$

where a_s is specific surface area of solid.

Liquid holdup is sensitive to the density and viscosity of the gas and liquid phases with varying extent. For example, holdup marginally changes with increase or decrease in liquid density or gas viscosity. However, it is considerably sensitive to the viscosity of the liquid phase and density of the gas phase. Liquid holdup is higher for viscous liquids and in such cases liquid–solid shear plays a greater role than the gas–liquid interactions. Most of the proposed correlations were expressed in terms of Reynolds number, which account for variation in the viscosity of the liquid or gas phase. Another important parameter that affects the liquid phase holdup is surface tension and foaming properties of the liquid phase. For liquid with surfactants, lowering the liquid surface tension enhances the spreading factor and liquid holdup decreases due to higher gas–liquid interaction. However, surface tension effects are considerable only for smaller-sized particles (1–2 mm) where capillary forces are

stronger in the small interstitial spaces. Liquid holdup can be related with surface tension property of liquid by means of Weber number. Correlation proposed by Clements (1978) and Clements and Schmidt (1980) has shown such dependency for low and high interaction regimes as:

$$\varepsilon\beta_{\mathrm{d}} = 0.111(We_{\mathrm{G}}Re_{\mathrm{G}}/Re_{\mathrm{L}})^{-0.034} \tag{26}$$

$$\beta_{\mathrm{d}} = 0.245(We_{\mathrm{G}}Re_{\mathrm{G}}/Re_{\mathrm{L}})^{-0.034} \tag{27}$$

Liquid holdup is also considerably sensitive to the operating pressure or gas density. Gas–liquid shear is higher for bed operating at elevated pressure which causes a decrease in liquid holdup. However, this effect is negligible at lower gas velocities ($V_{\mathrm{G}} < 0.01$–0.02 kg/m^{2}s) compared to the higher gas flow rates. At high pressure, liquid holdup decreases with increase in reactor operating pressure. Correlations proposed by Ellman, Midoux, Wild, Laurent, and Charpentier (1990) (Eq. (29)), Holub et al. (1992, 1993) (Eq. (19)), and Larachi et al. (1991) (Eq. (28)) are suitable for predicting liquid holdup at elevated pressures:

Larachi et al. (1991)

$$\log(1-\beta_{\mathrm{e}}) = -\frac{1.22We_{\mathrm{L}}^{0.15}}{Re_{\mathrm{L}}^{0.20}X_{\mathrm{G}}^{0.15}} \tag{28}$$

where, β_{e} is the external liquid saturation.

Ellman et al. (1990)

$$\log(\beta_{\mathrm{nc}}) = -RX_{\mathrm{G}}^{m}Re_{\mathrm{L}}^{n}We_{\mathrm{L}}^{p}\left(\frac{a_{\mathrm{v}}d_{\mathrm{k}}}{1-\varepsilon}\right)^{q},$$

$$\begin{aligned} &\text{For high interaction regime,} && R = 0.16,\ m = 0.325,\ n = 0.163,\\ &&& p = -0.13,\ \text{and}\ q = -0.163\\ &\text{For low interaction regime,} && R = 0.42,\ m = 0.24,\ n = 0.14,\\ &&& p = 0,\ \text{and}\ q = -0.14 \end{aligned} \tag{29}$$

a_{v} is the bed specific interfacial area and $d_{\mathrm{k}} = d_{\mathrm{p}}\sqrt[3]{16\varepsilon^3/9\pi(1-\varepsilon)^2}$.

Predicted liquid holdup values using above correlations are compared in Fig. 15. Correlation proposed by Ellman et al. (1990) predicts significantly higher holdup compared to the predictions using correlations by Holub et al. (1992), Larachi et al. (1991), and Wammes & Westerterp (1991). Accurate estimation of the liquid holdup is desired because it is one of the key parameters in the estimation of mean residence time and conversion in the reactor.

Wetting of the Catalyst Particles

In trickle bed reactors, extent of wetting of the catalyst particles (wetting efficiency) is another important parameter required for design calculations.

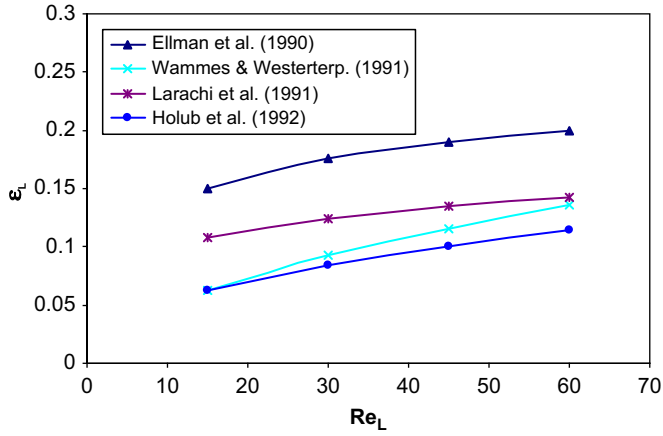

FIGURE 15 Comparison of predicted liquid holdup using various correlations for $U_G = 0.2$ m/s.

Among the various types of multiphase reactors, this phenomenon is unique in the trickle bed reactors and its quantification is a rather difficult task. Liquid flows non-uniformly over the catalyst particles leading to different degrees of wetting. Two types of wetting phenomenon are generally observed in the trickle bed reactors: external wetting of the catalyst particles and internal wetting of the particles. External wetting of the particles is a measure of fraction of catalyst surface covered by the liquid film, while internal wetting is the fraction of internal catalyst surface area covered by the liquid phase. In a trickle flow regime, external wetting is indispensable while in many situations internal wetting is not complete in spite of capillarity effects. Schematic of wetting behavior in trickle bed reactors is shown in Fig. 16. Three different wetting behaviors are observed viz., complete wetting, partial wetting, and incomplete internal wetting of particles.

External wetting can also affect some of the hydrodynamic properties in various ways and hence performance of the reactors. Presence of liquid film (like in trickle flow regime) over the catalyst surface restricts access of the gas phase reactants to the active sites. Partial wetting conditions have significant impact on the performance of the reactors. If the limiting reactant(s) is present in the liquid phase then reaction rates are directly proportional to the extent of wetting of the bed and hence partial wetting has negative effect on the performance of the reactor. If the limiting reactants are present in the gas phase, reaction rates get enhanced due to direct contact of gas phase reactants with active sites over the unwetted surface, since the catalyst particle is completely wetted internally due to capillary effects. In this case, particle wetting gives positive effect on the reactor performance. For volatile reactants, gas phase reaction can also be significant and in such a situation partial wetting was found to be beneficial. However, reaction rate analysis for such systems is fairly

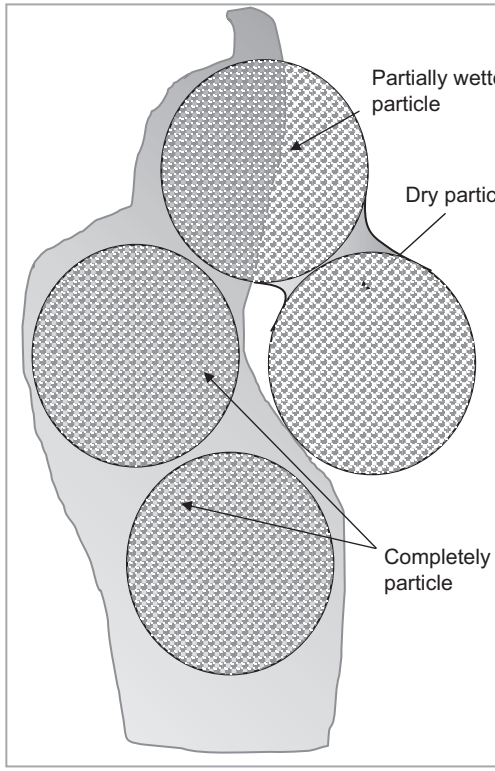

FIGURE 16 Wetting behavior of particles.

complex and requires accurate estimation of the wetted fraction. Operating parameters affecting the wetting and correlations for its accurate estimation are provided in the following.

Wetting efficiency of trickle bed reactors is defined as percent wetting of catalyst external surface area (Colombo, Baldi, & Sicardi, 1976; Herskowitz, Carbonell, & Smith, 1979; Schwartz, Weger, & Dudukovic, 1976). Measurement of wetting can be broadly categorized as direct measurement method and indirect measurement method. Photographic technique, dye injection method, computed tomography (CT) method, and magnetic resonance imaging (Sederman and Gladden, 2001) are some of the commonly used techniques for wetting efficiency. However, there are some indirect measurement techniques which are cost-effective as well as applicable for larger industrial units (for example, tracer techniques or methods based on reaction or mass transfer studies; by Colombo et al., 1976; Llano, Rosal, Sastre, & Díez, 1997, etc.). Although wetting phenomenon in trickle bed reactors is primarily governed by liquid throughputs (see Fig. 17), reactor hardware and operating parameters affect the wetting efficiency of trickle bed considerably and the effect of such parameters is discussed below.

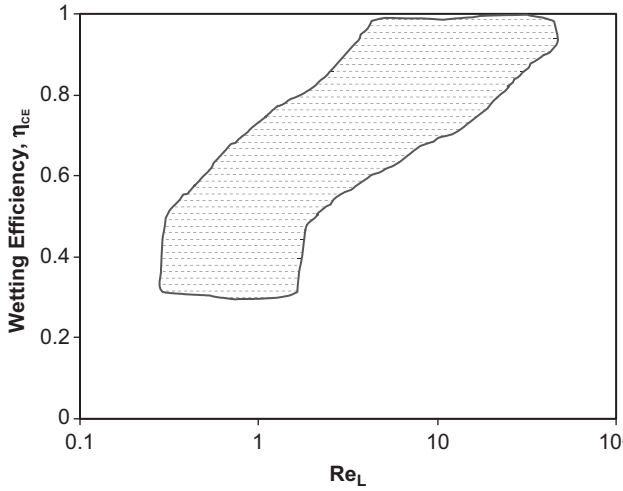

FIGURE 17 Typical variation of wetting efficiency with liquid phase Reynolds number (Herskowitz and Smith, 1983; Satterfield, 1975).

Reactor hardware, such as bed and particle diameter and porosity of bed, have significant effect on wetting efficiency of the bed. Apart from these parameters, liquid distributor is another parameter which affects wetting behavior indirectly. Non-uniform liquid distribution due to poor designing of distributor leads to liquid maldistribution. Some of the industrial-scale reactors are large in diameters (2−6 m diameter). For such large reactors, even a small variation in vertical orientation during installation of reactors leads to large-scale liquid maldistribution. Liquid maldistribution is directly related with wetting at least in a certain zone of the bed near the inlet; however, quantitative information on maldistribution is not readily available.

Apart from liquid maldistribution effects, particle diameter and porosity of the bed affect the wetting efficiency of the bed. Wetting efficiency decreases with increase in particle diameter. This trend can be attributed to two parameters: capillary pressure and liquid holdup. For smaller-sized particles, larger solid−liquid interaction leads to better spreading. Several studies reported this trend (Baussaron, Julcour-Lebigue, Wilhelm, Delmas, & Boyer, 2007; Dudukovic & Mills, 1986; El-Hisnawi, 1981). For trickle bed reactors where better wetting is critical, use of smaller-sized particles can improve wetting considerably at the expense of increase in pressure drop. Wu, Khadilkar, Al-Dahhan, and Dudukovic (1996) have suggested the use of inert fine particles along with catalyst particles to improve wetting efficiency without much increase in pressure drop. Effect of particle shape on wetting efficiency is negligible compared to the particle size (Al-Dahhan & Dudukovic, 1995; Baussaron et al., 2007). Correlations proposed by Burghardt et al. (1995) and

Mills and Duduković (1981) show the dependency of wetting efficiency on particle diameter.

$$\eta_{CE} = 1.0 - \exp\left(- 1.35 Re_L^{0.333} Fr_L^{0.235} We_L^{-0.17} \left(\frac{a_s d_p}{(1-\varepsilon_s)^2} \right)^{-0.0425} \right) \quad (30)$$

Or in terms of operating variables as:

$$\eta_{CE} = 0.038^* L^{0.22} G^{-0.083} d_p^{-0.373} \quad (31)$$

where, η_{CE} is external contacting efficiency, Fr is Froude number ($Fr = U^2/gd_p$), and ε_s is the solid holdup.

Besides particle diameter, external wetting efficiency is considerably sensitive to the gas−liquid flow rates. Most of the trickle bed reactors are operated at very low liquid mass flow rate (0.01−2 kg/m^{2}s). At such low liquid flow rates, liquid is insufficient to cover the catalyst surface and hence partial wetting is inevitable under such conditions. Effect of liquid flow rate is significant on wetting efficiency of the bed. Detailed analysis carried out by Sederman and Gladden (2001) shows that wetting efficiency initially changes at higher rate with liquid flow rate mainly because of the formation of new rivulets. It, however, reaches a saturation point where instead of formation of new rivulets, size of existing rivulets increases which improves wetting. Therefore, relative rate of increase of wetting efficiency is low at higher liquid throughputs. Dependency of wetting efficiency on liquid flow rate is represented by following correlations given by Alicilar et al. (1994), A.A. El-Hisnawi, Dudukovic, and Mills (1982), and A.E. El-Hisnawi, Dudukovic, and Mills (1982).

$$\eta_{CE} = 1.617 Re_L^{0.146} Ga_L^{-0.0711} \quad (32)$$

$$\eta_{CE} = 1 - \frac{25.6}{Re_L^{0.56}} \quad (33)$$

Not many studies have reported the effect of gas flow rate on wetting efficiency. Gas velocity shows different trends for variation in wetting efficiency. Two changes occur with increase in gas velocity viz., wetting efficiency decreases due to decrease in liquid holdup and wetting efficiency improves due to increase in gas−liquid shear. Negative effect of gas velocity is reported by Baussaron et al. (2007), Burghardt et al. (1995), Burghardt, Kolodziej, and Jaroszynski (1990), and Sederman and Gladden (2001) and they proposed the following correlation:

$$\eta_{CE} = 3.38^* Re_L^{0.22} Re_G^{-0.83} \left(d_p \sqrt{\frac{g\rho_L^2}{\mu_L^2}} \right)^{-0.512} \quad (34)$$

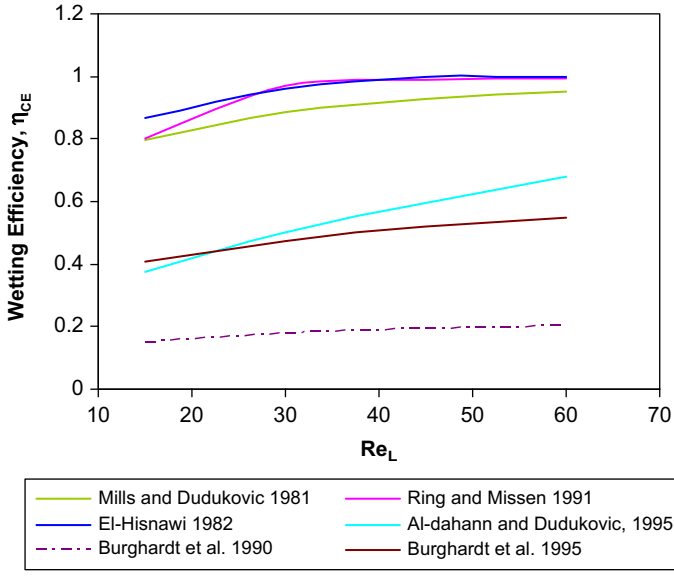

FIGURE 18 Wetting efficiency of particles predicted using various correlations.

Correlation proposed by Al-Dahhan and Dudukovic (1994) suggests an indirect effect of gas flow rate on wetting efficiency (Eq. 35). Their correlation for wetting efficiency is based on two-phase pressure drop which increases with gas flow rates and the experimental data collected at elevated operating pressure where one would expect higher gas−liquid shear:

$$\eta_{\mathrm{CE}} = 1.104 Re_{\mathrm{L}}^{0.33} \left[\frac{1 + [\Delta P/Z]/\rho_{\mathrm{L}} g}{Ga_{\mathrm{L}}} \right]^{1/9} \tag{35}$$

Very few studies have addressed the effect of gas density/operating pressure on wetting efficiency of the particles (Al-Dahhan & Dudukovic, 1995; Ring & Missen, 1991). Catalyst wetting efficiency improves with increase in operating pressure (higher density of gas leads to enhanced gas−liquid shear and therefore enhanced spreading of liquid).

Values of wetting efficiency calculated using various correlations are compared with each other in Fig. 18 (for trickle bed operated at atmospheric conditions and $Re_{\mathrm{G}} = 86.3$). Predictions based on the correlations proposed by A.A. El-Hisnawi, Dudukovic, and Mills (1982), A.E. El-Hisnawi, Dudukovic, and Mills (1982), Mills and Duduković (1981), and Ring and Missen (1991) lie close to each other. Predictions of correlations of Al-Dahhan and Dudukovic (1995) and Burghardt et al. (1995, 1990) are much lower than those predicted by these three correlations (and lower than the expected range of >0.6). Recently Baussaron et al. (2007) and Julcour et al. (2007) measured local and

average partial wetting efficiencies in trickle beds via direct measurements using image processing and PIV (particle image velocimetry). Such techniques along with MRI may provide better insight into partial wetting.

Gas–Liquid Mass Transfer Coefficient

Trickle flow operation is a rather "silent" class of operation as there is no rigorous mixing mechanism present like other multiphase catalytic systems as stirred tank, slurry bubble column reactors, or even like the high interaction flow regime. Therefore, mass transfer rates are lower than other reactors and often become rate-limiting in the performance of the trickle bed reactors. Many of the industrial reactions carried out in trickle bed reactors are reported to be falling under mass transfer-limiting conditions (for example, hydrogenation of α-methyl styrene and sulfur dioxide oxidation). Three types of mass transfer rates are relevant for trickle bed reactors, i.e., gas–liquid, liquid–solid, and gas–solid mass transfer rates. In gas–liquid mass transfer process, the liquid side mass transfer rate is often rate-limiting. Gas–liquid mass transfer rates are dependent on various system parameters such as particle diameter, gas–liquid flow rates, properties of fluids, and the reactor operating conditions. Based on these parameters several studies have reported correlations for gas–liquid mass transfer coefficients (see, for example, Cassanello, Larachi, Laurent, Wild, & Midoux, 1996; Charpentier & Favier, 1975; Fukushima & Kusaka, 1977b; Gianetto, Specchia, & Baldi, 1973; Larachi, Cassanello, & Laurent, 1998; Midoux, Morsi, Purwasasmita, Laurent, & Charpentier, 1984; Wammes & Westerterp, 1991; Wild, Larachi, & Charpentier, 1992). Key aspects are discussed in the following.

Reactor configuration (diameter, height) has rather limited role in altering gas–liquid mass transfer rates compared to the influence of particle size. The gas–liquid mass transfer rate increases with decrease in particle size. Two-phase pressure is an indication of extent of interaction among the flowing phases. For smaller-sized particles, this interaction is considerably higher and therefore the gas–liquid mass transfer rates. Some of the correlations of mass transfer include pressure drop (see, for example, a correlation proposed by Iliuta and Thyrion, 1997 which is reproduced here as Eq. (36)).

$$k_{GL}a_{GL} = 0.0036\left(\frac{U_L}{\varepsilon_{L,d}}\frac{\Delta P}{Z}\right)^{0.35} \tag{36}$$

where $\varepsilon_{L,d}$ is the dynamic liquid holdup.

Instead of expressing mass transfer correlation in terms of unknown pressure drop (which may have to be estimated using other correlations), Lange (1978) proposed a correlation based on known parameters as:

$$k_{GL}a_{GL} = 0.33D_{H_2,L}\left(\frac{d_R}{d_p}\right)^{0.46}\left(\frac{\rho_L u_L}{\mu_L}\right)^{0.14} Sc_{H_2L}^{0.5} \tag{37}$$

where D_{H_2L} is the diffusivity for hydrogen and $Sc_{H_2,L}$ is Schmidt number $(\mu_L \rho D_{H_2L})$.

Apart from particle size, gas–liquid mass transfer coefficient is also considerably sensitive to gas–liquid throughputs. Gas–liquid flow rate enhances the interaction between gas and liquid phases and spreading of liquid. This leads to an increase in gas–liquid interfacial area. Fig. 19 shows the variation of calculated mass transfer rates (based on the correlation proposed by Wild et al., 1992) with gas and liquid flow rates. The correlation proposed by Wild et al. (1992) is applicable for trickle, pulse, and transition flow regimes and is given below as Eqs. (38)–(40).

Low interaction regime:

$$\frac{k_{GL}a_{GL}d_k^2}{D_{AL}} = 2 \times 10^{-4}\left(X_G^{1/4} Re_L^{1/5} We_L^{1/5} Sc_L^{1/2}\left(\frac{a_v d_k}{1-\varepsilon}\right)^{1/4}\right)^{3.4} \tag{38}$$

High interaction regime:

$$\frac{k_{GL}a_{GL}d_k^2}{D_{AL}} = 0.45\left(X_G^{1/2} Re_L^{4/5} We_L^{1/5} Sc_L^{1/2}\left(\frac{a_v d_k}{1-\varepsilon}\right)^{1/4}\right)^{1.3} \tag{39}$$

Transition regime:

$$\frac{k_{GL}a_{GL}d_k^2}{D_{AL}} = 0.091\left(X_G^{1/4} Re_L^{1/5} We_L^{1/5} Sc_L^{3/10}\left(\frac{a_v d_k}{1-\varepsilon}\right)^{1/4}\right)^{3.8} \tag{40}$$

Gas–liquid mass transfer rates are also dependent on properties of the gas–liquid phases such as liquid phase surface tension and viscosity, diffusion

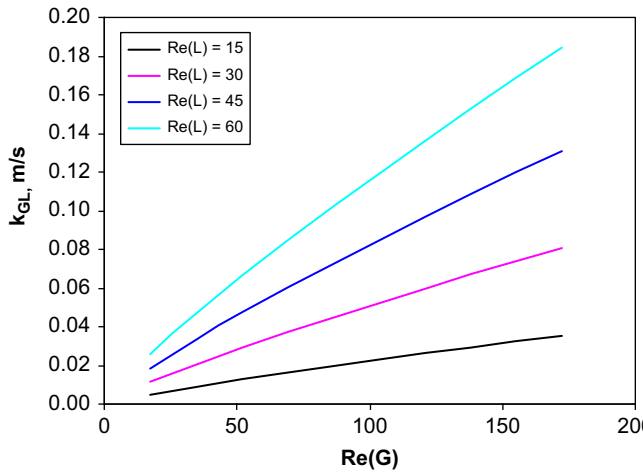

FIGURE 19 Typical variation of gas–liquid mass transfer coefficient with liquid phase Reynolds number (calculated based on Wild's correlation Eq. (38)).

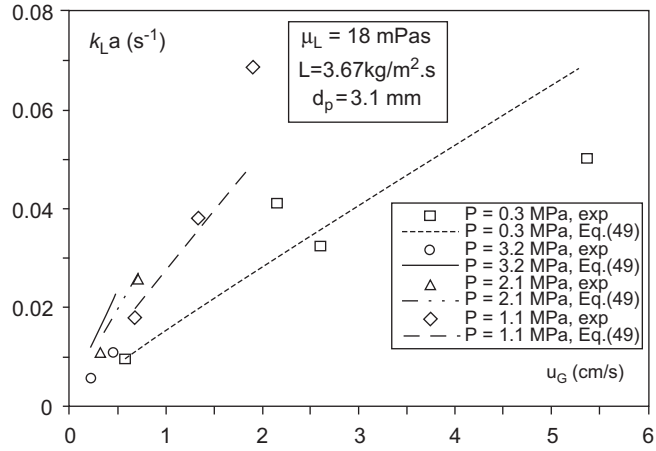

FIGURE 20 Effect of gas velocity and operating pressure on gas–liquid mass transfer coefficient (Larachi et al., 1998). System: ethylene triglycol + diethylamine 0.05 kmol, nitrogen gas with polypropylene extrudates of $d_p = 3.37$ mm [Eq.(49) in the legend refers to the equation number reported by Larachi et al. 1998].

coefficient, and gas phase density. Mass transfer rates are not very sensitive to parameters like gas phase viscosity and liquid density. Mass transfer rates vary considerably for foaming and non-foaming liquids. Foaming liquid leads to higher interfacial area and therefore higher mass transfer rates (Midoux et al., 1984; Morsi et al., 1982). For the case with foaming liquids, higher operating pressure suppresses foaming and leads to lower mass transfer rates. However, for the non-foaming liquids, operating pressure has relatively less influence on mass transfer rates. Increase in operating pressure or gas density enhances the mass transfer rates and this can be attributed to increase in gas holdup and interfacial area at high pressure (Larachi et al., 1998). At high operating pressure and moderate gas flow rate, gas phase penetrates into the liquid film in the form of tiny bubbles. This process increases the gas holdup as well as gas–liquid interfacial area. In addition to this, liquid spreading is higher at elevated operating pressure (Al-Dahhan & Dudukovic, 1994) which improves wetting as well as gas–liquid interfacial area. Experimental data collected by Larachi et al. (1998) demonstrate the effect of operating pressure on gas–liquid mass transfer rates; shown here as Fig. 20.

Liquid–Solid Mass Transfer Coefficient

Liquid–solid mass transfer is important for many trickle bed reactors and has been extensively studied (see, for example, Chou, Worley, & Luss, 1979; Kawase & Ulbrecht, 1981; Lakota & Levec, 1990; Latifi, Laurent, & Storck, 1988; Specchia, Baldi, & Gianetto, 1978). In trickle flow operations, liquid–solid mass transfer rates are dependent on the extent of liquid contact

with available solid surface. With increase in liquid flow rate, wetting behavior improves and therefore the liquid–solid mass transfer rates. Given the fact that wetting factor cannot be separated from mass transfer rates, several correlations, therefore, include the wetting factor as a parameter along with the liquid–solid mass transfer coefficient (see, for example, Chou et al., 1979; Latifi, Naderifar, Midoux, & Le Mehaute, 1994; Rao & Drinkenburg, 1985). Usually the liquid–solid mass transfer coefficient is expressed in terms of Schmidt number ($Sc = \mu/\rho D$) and Reynolds number ($Re = \rho U d_p/\mu$) with or without wetting factor as follows:

$$\eta_{CE} Sh = a(Re)^b Sc^{1/3} \tag{41}$$

where Sh is Sherwood number ($Sh = k_{LS} d_p/D$). Reported values of parameters appearing in this equation are listed in Table 2.

TABLE 2 Constants Proposed by Various Studies for Eq. (41) with Correction Factors

Author	η_{CE}	a	b	Other Factors
Chou et al. (1979)	0–1	0.43 0.72	0.22 0.54	$Re_L = Ko$ (high interaction regime) Extra term $Re_G^{0.16}$ (trickle flow regime)
Speechia et al. (1976)	1	2.79	0.7	$Re_L = Re_L/a_s$
Hirose et al. (1976)	1	8 0.53	0.5 58	$(Re_L < 200)$ $(Re_L > 200)$
Satterfield et al. (1978)	0–1	0.815	0.822	$Sh = Sh/(1-\varepsilon)$
Kawase and Ulbrecht (1981)	1	0.6875	0.33	–
Delaunay, Storck, Laurent, and Charpentier (1982)	0–1	1.84	0.48	–
Tan and Smith (1982)	1	4.25	0.48	–
Rao and Drinkenburg (1985)	0–1	0.24	0.75	$Re_L = Re_L/\varepsilon_L$
Latifi et al. (1988)	1	1.2	0.533	$Sh = Sh[\varepsilon_B/(1-\varepsilon_B)]$
Lakota and Levec (1990)	1	0.847	0.495	$Re_L = Re_L(\varepsilon_B/h_d)/(1-\varepsilon_B)$

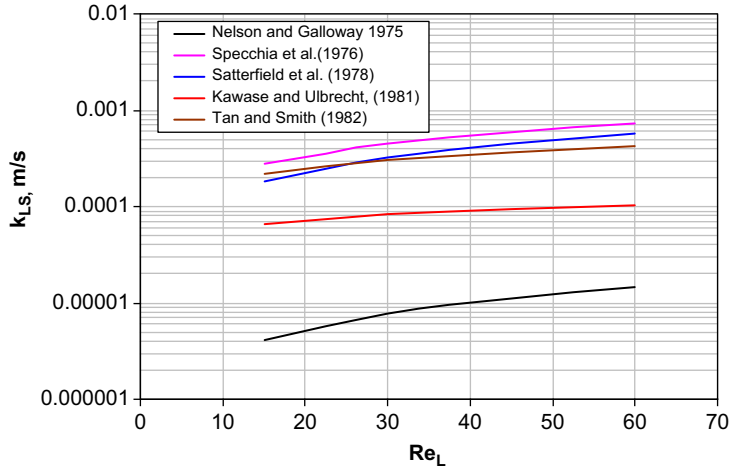

FIGURE 21 Comparison of prediction of liquid–solid mass transfer coefficient using correlations proposed by various studies.

Nelson and Galloway (1975) reported the effect of reactor and particle diameter on liquid–solid mass transfer coefficient as:

$$k_{\mathrm{LS}}a_{\mathrm{S}}\varepsilon_{\mathrm{S}} = 0.75D_{\mathrm{H_2,L}}\left(\frac{d_{\mathrm{R}}}{d_{\mathrm{p}}}\right)^{0.82}\left(\frac{\rho_{\mathrm{L}}u_{\mathrm{L}}}{\mu_{\mathrm{L}}}\right)^{0.9}Sc_{\mathrm{H_2L}}^{0.5} \tag{42}$$

Liquid–solid mass transfer rate is quite sensitive to particle diameter and increases with decrease in particle size (Goto & Smith, 1975; Hirose, Mori, & Sato, 1976; Specchia et al., 1978). Liquid–solid mass transfer rates are considerably sensitive to the liquid mass flow rates compared to the gas mass flow rates. Mass transfer rate increases with liquid mass flow rates and significant enhancement is observed at lower liquid flow rates than higher. Highfill and Al-Dahhan (2001) have shown that mass transfer rates are higher at the central portion of the column where liquid flow rates are supposed to be higher because of segregation. Gas phase has negligible effect on liquid–solid mass transfer rates and Specchia et al. (1978) have reported that these effects are considerable only at low gas flow rates. Comparison of predicted values of liquid–solid mass transfer coefficients by different correlations as a function of liquid phase Reynolds number is shown in Fig. 21.

Gas–Solid Mass Transfer

Gas–solid mass transfer coefficient is required in modeling of trickle bed reactor when catalyst particles are partially wetted. On the dry surface of the catalyst particle, there is a direct contact between gas phase reactants and the external catalyst surface. Gas–solid mass transfer has been extensively studied

in single-phase reacting systems. Two key correlations are included here which may be used to estimate gas−solid mass transfer coefficients:

Nelson and Galloway (1975):

$$k_{GS} = 0.18\left(\frac{D_{H_2,\,G}}{d_p}\right)\varepsilon_s^{0.33}\left(\varepsilon_s^{-0.33} - 1\right)(Re_G)\left(Sc_{H_2,G}^{2/3}\right) \tag{43}$$

Dwivedi and Upadhyah (1977):

$$k_{GS} = 0.4548\left(\frac{H_A u_G}{\varepsilon_B}\right)(Re_G)^{-0.4069}\left(Sc_G^{-0.667}\right) \tag{44}$$

Axial Dispersion

Liquid distribution and mixing are other important parameters in the design of trickle bed reactors. Main factors contributing to liquid distribution and back mixing are non-uniform porosity distribution, capillarity action, dead-zones, partial wetting, and channeling or short-circuiting. These factors exhibit strong interaction among themselves and encompass wide range of spatio-temporal scales (micro-scale, meso-scale, and macro-scale). Therefore quantification of individual factors on mixing and on non-ideal flow behavior is rather a challenging task. Measurement of residence time distribution (RTD) is one of the oldest (Danckwerts, 1953) and successful methods for characterizing such flow non-idealities. Measurement of RTD is relatively straightforward compared to the processing and interpretation of RTD data. Commonly used practice is to interpret the RTD data obtained for trickle bed reactors with the axial dispersion model (ADM) which lumps all flow non-idealities into a single-fitted parameter called dispersion coefficient (D_L).

As mentioned earlier, flow non-idealities in trickle bed reactors occur due to combined effect of several macro-scale and micro-scale processes. It is possible to elicit the effect of macro-scale and micro-scale flow processes to some extent using variants of ADM models which are composed of more than one fitted parameter (2−6 parameters). Immediate extension of such a model is possible by splitting the dispersion coefficient into axial and radial directions (multistage dispersion model (MDM) or mixing cell model, Ramachandran & Smith, 1979). Other versions of ADM by considering random delay of fluid element due to travel in packed bed (probabilistic time model [PTB] of Buffman, Gibilaro, & Rathor, 1970) or by considering the effects of mass exchange between static and dynamic regions along with back mixing of fluid (of Van Swaaij, Charpentier, & Villermaux, 1969) have also been used. If porous particles are present in the system, dynamics of the trickle bed reactors is altered by additional lag due to associated diffusion, adsorption, and desorption processes (Iliuta & Larachi, 1999). Despite a wide variety of models, single parameter ADM is the most widely used model for characterizing system

non-idealities because of its simplicity. Variation of the dispersion coefficient (in terms of Peclet number, Pe_L or Bodenstein number, Bo) with system parameters is discussed in the following.

Liquid phase Peclet number (Pe_L defined as $U_L D/D_L$) depends on key reactor parameters such as reactor diameter, length, particle diameter, and porosity. Mears (1971) has proposed a criterion to identify whether dispersion is relevant based on conversion of a reactant and the Peclet number. This criterion states that minimum reactor length required for ignoring dispersion effects as:

$$\frac{z}{d_p} > \frac{20n}{Pe_L} \ln\left(\frac{C_{in}}{C_{out}}\right) \tag{45}$$

where, n is the reaction order, C is the concentration, and z is the reactor length. Above expression indicates that dispersion effects are considerable for higher conversions or higher order of reactions and lower Peclet numbers. Apart from reactor length, particle diameter has also significant effect on dispersion at lower liquid flow rates. Study of Fu and Tan (1996) shows that dispersion is sensitive to particle diameter at low liquid flow rates ($Re_L < 4$) and almost independent of particle diameter for higher liquid flow rates. Following correlation is proposed for low liquid flow rates,

$$Bo = 0.00014(d_h)^{-0.75}(\varepsilon)^{-1} \tag{46}$$

where Bo is the Bodenstein number ($Bo = (Uz/D_{ax})$) and d_h is the hydraulic diameter and D_{ax} and z are dispersion coefficient and length of the column, respectively.

Pant, Saroha, & Nigam, (2000) have shown that dispersion varies considerably with shape of the particles especially with increase in liquid flow rates. For extrudates, dispersion remains unchanged for a range of Reynolds numbers ($Pe_L = 30$, for $Re_L = 24{-}94$). However, it changes considerably for glass beads and tablets ($Pe_L = 50{-}200$) for the same range of Reynolds number. Besides particle size and shape, particle porosity has also significant effect on dispersion number (Iliuta, Thyrion, & Muntean, 1996; Saroha, Nigam, Saxena, & Kapoor, 1998). Dispersion coefficient is found to be lower for porous particles than non-porous particles.

Effect of gas flow rate on dispersion coefficient is almost negligible and several studies have reported this trend (Cassanello, Martinez, & Cukierman, 1992; Pant et al., 2000; Saroha et al., 1998; Tosun, 1982). Quantitative dependency on gas flow rate is given by Hochman and Effron (1969) in the form of following correlation:

$$Pe_L = 0.034(Re_L)^{0.5} 10^{0.008 Re_G} \tag{47}$$

Effect of liquid flow rate is significant on dispersion coefficient especially for lower liquid flow rates ($Re_L < 50$). Figure 22 shows the residence time

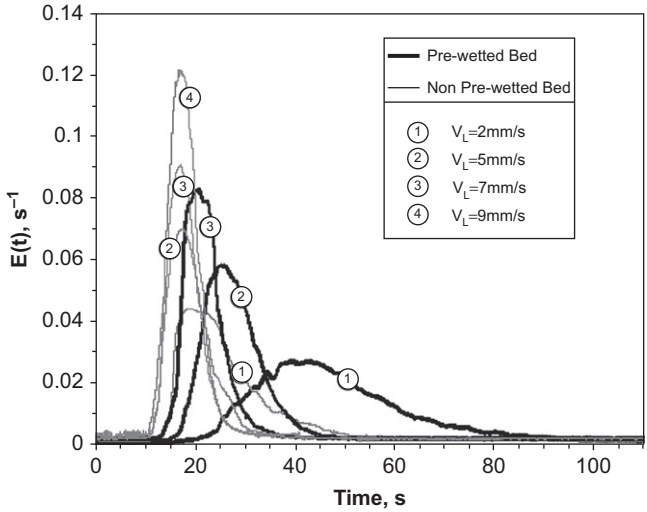

FIGURE 22 Effect of bed prewetting on dispersion behavior of trickle bed reactors (Gunjal et al., 2003). System: $D = 0.114$ m, $d_p = 3$ mm glass sphere.

distribution plots for air–water system at different liquid flow rates which clearly indicate the importance of dispersion at low liquid flow rates. This figure also demonstrates that beside liquid flow rates, bed prewetting conditions (capillary pressure) have significant effect on dispersion of liquid phase at lower liquid flow rates. Dependency of dispersion on liquid flow rates can be expressed in terms of liquid phase Reynolds number. Matsuura, Takashi, and Takashi (1976) have shown that dispersion is independent of Reynolds number for very low liquid flow rates ($Re_L < 4$) and then increases linearly with Re_L.

$$\begin{aligned} Bo &= 0.43, \quad \text{for } Re_L < 150 \\ Bo &= 1.7, \quad \text{for } Re_L > 400 \\ Bo &= 0.0052Re_L - 0.332, \quad \text{for } 150 > Re_L > 400 \end{aligned} \tag{48}$$

The generalized form of the correlation for liquid phase dispersion coefficient is

$$Bo = a(Re_L)^b(Ga_L)^c \tag{49}$$

Exponent of Reynolds number was found to be in the range of 0.3–0.6 while the exponent of Galileo number was found to be in the range of 0.2–0.7. Some of the published values of these parameters are listed in Table 3.

Dispersion effects in gas–liquid trickle flow through packed bed are significantly higher than that in single-phase flow through packed bed ($Bo = 0.5$ and 0.1 for single-phase flow and trickle flow, respectively). The

TABLE 3 Correlations for Dispersion Coefficient Proposed by Various Studies

Author	Correlations for Dispersion Number
Otake and Kunugita (1958)	$Bo = 1.9(Re_L)^{0.5}(Ga_L)^{-0.333}$
Hochman and Effron (1969)	$Pe_L = 0.042(Re_L)^{0.5}$, $4 < Re_L < 100$
Michell and Furzer (1972)	$Pe_L = (Re_L/\varepsilon)^{0.7}(Ga_L)^{-0.32}$, $50 < Re_L < 1000$
Turek, Lange, and Bush (1979)	$Bo = 0.034(Re_L)^{0.53}$
Buffham and Rathor (1978)	$Pe_L = 60(Re_L)^{0.63}(Ga_L)^{-0.73}$
Kobayashi, Kushiyama, Ida, and Wakao (1979)	$Pe_L = 60(Re''_L)^{0.63}(Ga''_L)^{-0.73}$
Cassanello et al. (1992)	$Bo = 2.3(Re_L)^{0.33}(Ga_L)^{-0.19}$
Wanchoo, Kaur, and Bansal (2007)	$Bo = 0.4548(Re_L)^{0.55}$, $4 < Re_L < 80$

dispersion effects in trickle bed reactors therefore cannot be neglected especially for low liquid flow rates, smaller length column, and higher conversions.

Heat Transfer in Trickle Bed Reactors

Most of the reactions carried out in trickle bed reactors are exothermic in nature (e.g., hydrogenation, oxidation, and hydrotreating). Removal of heat liberated due to chemical reactions from reactor becomes necessary to avoid catalyst deactivation/sintering and for safer operation. Trickle bed reactors are prone to temperature runaway conditions due to poor heat transfer rates. Therefore, operating trickle bed reactors under adiabatic conditions is one of the major challenges. Temperature uniformity in the reactor is desired in order to achieve better selectivity, product uniformity, and quality. This can be achieved by removing heat either via cooling coils or intermediate quenching, or using low boiling solvent. In trickle bed reactors, large radial temperature non-uniformities are observed and several studies have reported hotspot formation and runaway conditions (see, for example, Germain, Lefebvre, & L'Homme, 1974; Hanika, 1999; Jaffe, 1976; Weekman, 1976). Accurate estimation of heat transfer rates is therefore critical for successful design and scale-up of trickle bed reactors. Key parameters affecting heat transfer in trickle beds are discussed in the following.

Heat transfer in trickle bed reactor occurs at various levels:

- heat transfer inside the catalyst pellets where reactions occur (intraparticle heat transfer),
- heat transfer from pellet to the surrounding fluid (particle—fluid heat transfer),

- heat transfer from pellets to pellets (interparticle heat transfer), and
- heat transfer from bed to the wall of the reactor.

Considering the internal wetting and presence of liquid in the pores, in many cases, temperature is reasonably uniform inside the catalyst particle. Many studies have reported particle−fluid heat transfer coefficient for single-phase flow (see, for example, Achenbach, 1995; Briens, Del Pozo, Trudell, & Wild, 1999; Ranz, 1952, and the references cited therein). Relatively very few studies have been reported on particle−fluid heat transfer rates for trickle flow operation (see, for example, Boelhouwer, Piepers, & Drinkenburg, 2001; Marcandelli, Wild, Lamine, & Bernard, 1999). Most of the earlier studies were focused on calculating effective axial and radial heat transfer coefficients (Chu & Ng, 1985; Matsuura, Hitaka, Akehata, & Shirai, 1979; Specchia et al., 1979; Weekman & Myers, 1965) and the bed to wall heat transfer coefficients (Muroyama, Hashimoto, & Tomita, 1977; Specchia et al., 1979). Various heat transfer modes and their relationship with key parameters of trickle bed reactors are briefly discussed in the following.

Particle−fluid heat transfer coefficient is a function of gas and liquid phase velocities and thermal properties of the fluids and particles (that is, thermal conductivity of liquid, density, and viscosity of the liquid and thermal conductivity of the solids). Particle−fluid heat transfer coefficient is independent of reactor diameter. Dimensionless analysis suggests the following relationship for heat transfer coefficient and operating parameters:

$$Nu = a(Re)^b Pr^{1/3} \tag{50}$$

Boelhouwer et al. (2001) have measured heat transfer rates in 0.11 diameter column filled with 6 mm glass beads for air−water system and suggested values of $a = 0.111$ and $b = 0.8$ for trickle as well as pulse flow regimes. In pulse flow regime heat transfer rates are higher than the trickle flow regime. Detailed measurements by Boelhouwer et al. (2001) and Huang, Varma, and McCready (2004) indicate that higher liquid phase velocity is beneficial for dissipating heat from the catalyst particles in a pulse flow regime. Heat transfer rates during the passage through liquid rich zones are 3−4 times higher than passage of liquid lean zones. Figure 23 shows experimentally measured heat transfer coefficient in the liquid-rich zone of pulse flow and the base region at different gas and liquid velocities. Studies of Boelhouwer et al. (2001) also indicated that the heat transfer rates at the center of the column are lower (1.5−2.5 times) compared to the periphery of the column. This effect is attributed to the packing density and local liquid velocities.

Heat transfer was found to increase with gas as well as liquid flow rates (Boelhouwer et al., 2001; Marcandelli et al., 1999). A sample of results of Boelhouwer et al. (2001) is shown in Fig. 24. However, heat transfer rate enhancement due to increased gas flow rates is rather marginal compared to the enhancement due to increased liquid flow rates.

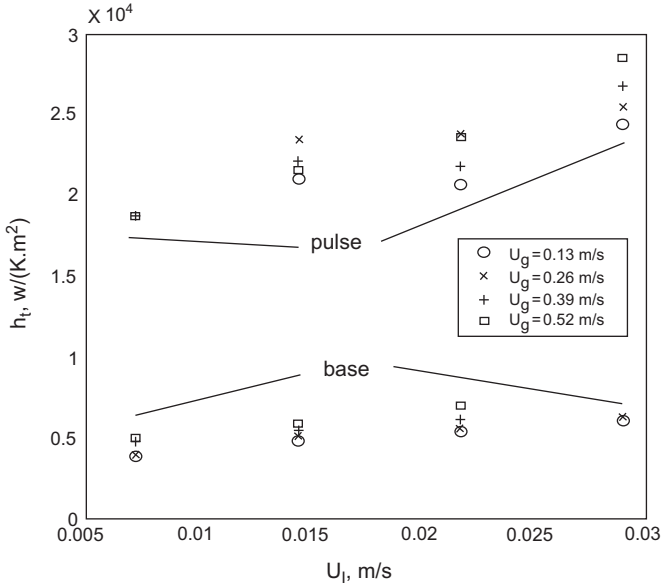

FIGURE 23 Experimental data on heat transfer coefficient measured in the liquid-rich and lean zones by Huang et al. (2004). System: $D = 7.4$ cm, $d_p = 6-8$ mm glass sphere.

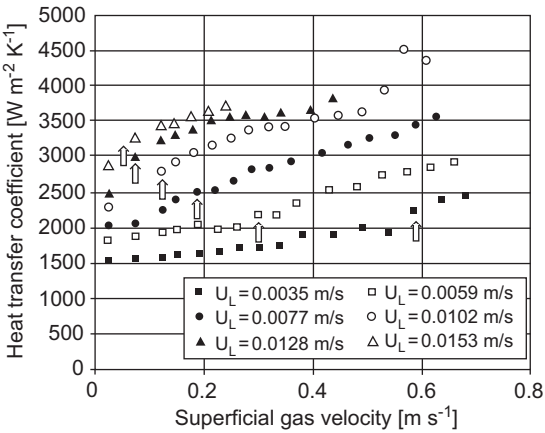

FIGURE 24 Experimental data on heat transfer coefficient at different gas and liquid velocities (Boelhouwer et al., 2001). System: $D = 0.11$ m, $d_p = 6$ mm glass sphere, $\varepsilon = 0.38$.

Effective thermal conductivity of the bed is a measure of the average thermal conductivity of the bed in the presence of gas and liquid phases in axial as well as radial directions. Most of the previous studies have focused on the effective radial thermal conductivity of the bed because of relatively higher temperature gradients in the radial direction than in the axial direction. Hashimoto, Muroyama, Fujiyoshi, and Nagata (1976) and Weekman and Myers

(1965) have related the effective radial thermal conductivity (Λ_r) to the liquid thermal conductivity and the bed properties (porosity (ε) and diameter of bed (D) and particle (d_p)) along with liquid phase Peclet (Pe_l) number and dynamic liquid holdup (β_l) in the form of following correlation:

$$\frac{\Lambda_r}{\lambda_l} = \frac{12.2}{\lambda_l} + \frac{0.000285}{\varepsilon}\frac{D}{d}\frac{Pe_l}{\beta_l} \tag{51}$$

where λ is the thermal conductivity of liquid and Pe_l is the liquid Peclet number ($Pe_l = LC_{pl}d_p/k_l$).

In addition to these parameters, Hashimoto et al. (1977) have also taken convective term into account in the form of liquid phase Reynolds number (Re_l) as follows:

$$\frac{\Lambda_r}{\lambda_l} = \frac{0.465}{\lambda_l} + \alpha_l Re_l Pr_l + 0.110\frac{GC^*_{pg}d}{\lambda_l}$$
$$\alpha_l = \left[\frac{1}{1.9 + 0.0264(DL/\varepsilon\beta_l\mu_l)}\right]\frac{2\varepsilon}{3(1-\varepsilon)} \tag{52}$$

where C^*_{pg} is heat capacity of saturated gas.

Specchia and Baldi (1979) suggested that thermal conductivity of air and solid also needs to be accounted along with the contribution due to the gas and liquid flows. They have defined the effective radial conductivity as:

$$\Lambda_r = \lambda^o_e + \lambda_{e,g} + \lambda_{e,l} \tag{53}$$

where, λ^o_e is the bed thermal conductivity in the absence of any flow and $\lambda_{e,g}$ and $\lambda_{e,l}$ are contributions due to gas and liquid flows. With these parameters following correlation is suggested:

$$\frac{\Lambda_r}{\lambda_l} = \frac{\lambda_{SO}}{\lambda_l} + \frac{GC^*_{pg}d}{K\lambda_l} + \frac{\lambda_{rl}}{\lambda_l}, \tag{54}$$

where constants are

$$K = 8.65((1 + 19.4)(d/D)^2)$$
$$\frac{\lambda_{SO}}{\lambda_l} = \varepsilon + \frac{(1-\varepsilon)\lambda_g/\lambda_l}{0.22\varepsilon^2 + (2\lambda_g/3\lambda_S)}$$
$$\frac{\lambda_{rl}}{\lambda_l} = 24.4(\varepsilon\beta_l)^{0.87}Re_l^{0.13}Pr_l \tag{55}$$

Effective bed thermal conductivity increases with decrease in particle diameter. Effective bed conductivity depends on dynamic liquid holdup. Dynamic liquid holdup increases with liquid flow rate and decreases with gas flow rate. Data from the study of Lamine, Gerth, Legall, and Wild (1996) are shown in Fig. 25. It can be seen that the effective bed conductivity remains more or less constant in the trickle flow regime and increases as it approaches the

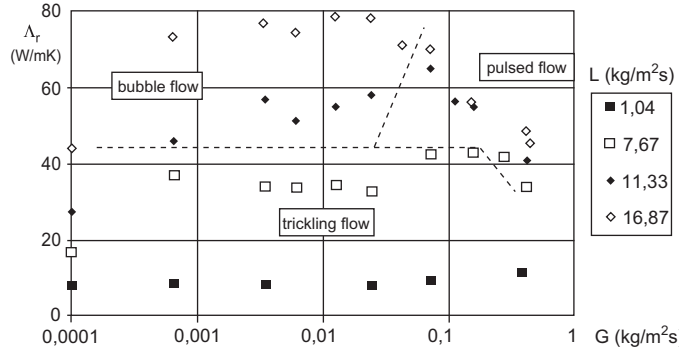

FIGURE 25 Experimental data on effective radial heat transfer coefficient at different gas and liquid velocities (Lamine et al., 1996). System: $D = 0.1$ m, $d_p = 6$ mm, air−water.

pulse flow regime. Effective thermal conductivity for the bubbly flow regime is higher than trickle flow mainly because of higher dynamic liquid holdup.

Wall to bed heat transfer rate is strongly dependent on distribution of liquid and wall flow characteristics. In trickle bed reactor, complete wetting of wall occurs occasionally and heat transfer rates are dependent upon liquid wall flow velocities. Muroyama et al. (1977) have related wall heat transfer to the liquid phase Reynolds number and Prandtl number as:

$$Nu = 0.012 Re_l^{1.7} Pr_l^{0.33} \tag{56}$$

Their study also suggests that heat transfer coefficient in the high interaction regime is a function of dynamic liquid holdup and can be predicted by the following correlation:

$$Nu = 0.092 \left(\frac{Re_l}{\varepsilon \beta_l}\right)^{0.8} Pr_l^{0.33} \tag{57}$$

Specchia et al. (1979) proposed a similar correlation except that in the high interaction regime, it remained unaffected by operating parameters as:

$$Nu = 0.057 \left(\frac{Re_l}{\varepsilon \beta_l}\right)^{0.89} Pr_l^{0.33}, \quad \text{for low interaction regime} \tag{58}$$

$$h_w = 2100 \text{ W/m}^2\text{K}, \quad \text{for high interaction regime} \tag{59}$$

It may be noted from the discussions so far that most of the key hydrodynamic parameters interact with each other and therefore interdependent. Estimation of one hydrodynamic parameter often required estimation of other related parameters. It is therefore essential to understand implications of possible errors associated with the estimated quantities and consequences of this on subsequent usage for estimation of other related parameters. The

sequence in which these different parameters are estimated may often turn out to be important. The discussion in this chapter was organized to indicate one such sequence (from flow regimes to heat transfer). However, more often than not, iterative procedure is used and multiple ways are used to cross-check and ensure consistency in the estimated values of key hydrodynamic parameters. Variety of other factors like closeness of considered system and operating conditions with those used for developing correlations, purpose of estimation, error bars associated with the data used while developing correlations, and prior experience determine the selection of particular set of correlations and methodology for estimating the required set of hydrodynamic parameters.

SUMMARY

Accurate estimation of hydrodynamic parameters is an indispensable step for the reactor design, performance evaluation, and scale-up studies. Hydrodynamics of trickle bed reactors is controlled by complex internal bed structure and associated interactions with the gas and liquid flows. The first step in estimating the hydrodynamic parameters is estimation of prevailing flow regimes under the operating conditions. The correlations and discussion presented in *Flow Regimes* are useful for selection of criteria to evaluate the flow regime and its transition so that all further calculations will be based on characteristics of that flow regime. Trickle bed reactors are often operated near the boundary of trickle and pulse flow regimes in practice. It is therefore important to be able to estimate the transition boundary between trickle and pulse regimes accurately. The methods and models presented in *Flow Regime Transition* can be used to determine transition boundary. Methods and correlations for estimating other key hydrodynamic parameters such as pressure drop, liquid holdup, mass and heat transfer coefficients, and axial dispersion are discussed in *Estimation of Key Hydrodynamic Parameters.*

It is important to note that the hydrodynamics of trickle beds is a complex function of interactions of particle properties, packing characteristics of the bed, properties of gas and liquid, and operating conditions. Therefore, literature data when correlated for particular parameters give considerably different values for same operating parameters. Error bar for experimentally measured values and the predicted ones using various correlations is anywhere between $\pm 15\%$ and $\pm 60\%$. It is often necessary to extrapolate the results of correlations or models to conditions beyond those considered during their development. It is critical in such cases to use multiple models and correlations and compare their extrapolated results to draw appropriate conclusions. Accumulated experience and application of the computational fluid dynamic models (discussed later in Chapter 4) are often used to guide such extrapolation exercise. It is also important to assess the sensitivity of predictions of reactor models and key engineering conclusions with variation of the estimated values of design

parameters. Such assessment may provide guidelines for determining desired accuracy and precision required while estimating these design parameters.

The methods, correlations, and models discussed here will be useful to complement the reaction engineering and computational fluid dynamics models of trickle bed reactors discussed in the following chapters.

REFERENCES

Achenbach, E. (1995). Heat and flow characteristics of packed bed. *Experimental Thermal and Fluid Science, 27*, 10–17.

Alicilar, A., Bicer, A., & Murathan, A. (1994). The relation between wetting efficiency and liquid holdup in packed columns. *Chemical Engineering Communications, 128*, 95–107.

Al-Dahhan, M. H., & Dudukovic, M. P. (1994). Pressure drop and liquid holdup in high pressure trickle-bed reactors. *Chemical Engineering Science, 49*, 5681–5698.

Al-Dahhan, M. H., & Dudukovic, M. P. (1995). Catalyst wetting efficiency in trickle-bed reactors at high pressure. *Chemical Engineering Science, 50*(15), 2377–2389.

Attou, A., & Ferschneider, G. (2000). A two-fluid hydrodynamic model for the transition between trickle and pulse flow in a co-current gas–liquid packed-bed reactor. *Chemical Engineering Science, 5*, 511–5491.

Baker, O. (1954). Simultaneous flow of oil and gas. *Oil and Gas Journal, 53*, 185.

Bansal, A., Wanchoo, R. K., & Sharma, S. K. (2005). Flow regime transition in a trickle bed reactor. *Chemical Engineering Communications, 192*, 1046–1066.

Baussaron, L., Julcour-Lebigue, C., Wilhelm, A., Delmas, H., & Boyer, C. (2007). Wetting topology in trickle bed reactors. *AIChE Journal, 53*(7), 1850–1860.

Benkrid, K., Rode, S., & Midoux, N. (1997). Prediction of pressure drop and liquid saturation in trickle-bed reactors operated in high interaction regimes. *Chemical Engineering Science, 52*, 4021–4032.

Boelhouwer, J. G., Piepers, H. W., & Drinkenburg, A. A. H. (2001). Particle–liquid heat transfers in trickle-bed reactors. *Chemical Engineering Science, 56*, 1181–1187.

Boelhouwer, J. G., Piepers, H. W., & Drinkenburg, A. A. H. (2002). Nature and characteristics of pulsing flow in trickle-bed reactors. *Chemical Engineering Science, 57*, 4865–4876.

Briens, C. L., Del Pozo, M., Trudell, C., & Wild, G. (1999). Measurement and modeling of particle–liquid heat transfer in liquid–solid and gas–liquid–solid fluidized beds. *Chemical Engineering Science, 54*, 731–739.

Buffman, B. A., Gibilaro, L. G., & Rathor, M. N. (1970). A probabilistic time delay description of flow in packed beds. *AIChE Journal, 16*, 218–223.

Buffham, B. A., & Rathor, M. N. (1978). The influence of viscosity on axial mixing in trickle flow in packed bed. *Transactions of Institute of Chemical Engineering,* London*, 56*, 266.

Burghardt, A., Bartelmus, G., Jaroszynski, M., & Kolodziej, A. (1995). Hydrodynamics and mass transfer in a three-phase fixed-bed reactor with cocurrent gas–liquid downflow. *Chemical Engineering Journal and the Biochemical Engineering Journal, 58*(2), 83.

Burghardt, A., Bartelmus, G., & Szlemp, A. (2004). Hydrodynamics of pulsing flow in three-phase fixed-bed reactor operating at an elevated pressure. *Industrial and Engineering Chemistry Research, 43*, 4511–4521.

Burghardt, A., Kolodziej, A., & Jaroszynski, M. (1990). Experimental studies of liquid–solid wetting efficiency in trickle bed cocurrent reactors. *Chemical Engineering and Processing, 18*, 35–49.

Cassanello, M., Larachi, F., Laurent, A., Wild, G., & Midoux, N. (1996). Gas−liquid mass transfer in high pressure trickle-bed reactors: experiments and modeling. In Ph. Rudolf von Rohr, & Ch. Trepp (Eds.), *Proceedings of the third international symposium on high pressure chemical engineering, Zurich, Switzerland, Oct 7−9, Vol. 12* (pp. 493). Amsterdam, The Netherlands: Elsevier B.V.

Cassanello, M. C., Martinez, O. M., & Cukierman, A. L. (1992). Effect of the liquid axial dispersion on the behavior of fixed bed three phase reactors. *Chemical Engineering Science, 47*(13−14), 3331−3338.

Charpentier, J.-C., Bakos, M., & Le Goff, P. (1971). Hydrodynamics of two-phase concurrent downflow in packed-bed reactors. Gas−liquid flow regimes. Liquid axial dispersion and dead zones. *Proceedings of the Second Congress Applied Physical Chemistry, 2*, 31−47.

Charpentier, J. C., & Favier, M. (1975). Some liquid holdup experimental data in trickle-bed reactors for foaming and nonfoaming hydrocarbons. *AIChE Journal, 21*, 1213−1218.

Charpentier, J. C., Prost, C., & Le Goff, P. (1969). NonEnChute de Pression pour des écoulements à cocourant dans des colonnes à garnissage arrosé: comparaison avec le garnissage noyé. *Chemical Engineering Science, 24*, 1777−1794.

Chhabra, R. P., Comiti, J., & Machac, I. (2001). Flow of non-Newtonian fluids in fixed and fluidized bed. *Chemical Engineering Science, 56*, 1−27.

Chou, T. S., Worley, F. L., & Luss, D., Jr. (1977). Transition to pulsed flow in mixed-phase cocurrent downflow through a fixed bed. *Industrial and Engineering Chemistry Process Design and Development, 16*, 424−427.

Chou, T. S., Worley, F. L., Jr., & Luss, D. (1979). Local particle−liquid mass transfer fluctuations in mixed-phase co-current down flow through a fixed bed in the pulsing regime. *Industrial and Engineering Chemistry Fundamentals, 18*, 279.

Chu, C. F., & Ng, K. M. (1985). Effective thermal conductivity in trickle-bed reactors: application of effective medium theory and random walk analysis. *Chemical Engineering Communications, 37*, 127−140.

Clements, L. D. (1978). Dynamic liquid holdup in cocurrent gas−liquid downflow in packed beds, 1. In T. N. Veziroglu, & S. Kakac (Eds.), *Phase transport and reactor safety.* Washington: Hemisphere Publ. Corp.

Clements, L. D., & Schmidt, P. C. (1980). Dynamic liquid holdup in two-phase downflow in packed beds: air−silicone oil systems. *AIChE Journal, 26*, 317−319.

Colombo, A. J., Baldi, G., & Sicardi, S. (1976). Solid−liquid contacting effectiveness in trickle-bed reactors. *Chemical Engineering Science, 31*, 1101.

Danckwerts, P. V. (1953). Continuous flow systems. Distribution of residence times. *Chemical Engineering Science, 2*, 1−13.

Delaunay, C. B., Storck, A., Laurent, A., & Charpentier, J. C. (1982). Electrochemical determination of liquid−solid mass transfer in a fixed bed irrigated gas−liquid reactor with downward co-current flow. *International Chemical Engineering, 22*(2), 244−251.

Duduković, M. P. (1977). Catalyst effectiveness factor and contacting efficiency in trickle-bed reactors. *AIChE Journal, 23*, 940−944.

Dudukovic, M. P. (2000). Opaque multiphase reactors: experimentation, modeling and troubleshooting. *Oil & Gas Science and Technology − Rev. IFP, 55*(2), ,135−158.

Dudukovic, M. P., & Mills, P. L. (1986). Contacting and hydrodynamics in trickle-bed reactors. In N. P. Cheremisinoff (Ed.), *Encyclopedia of fluid mechanics: gas−liquid flows, Vol. 3* (pp. 969). Houston, TX: Gulf Publ. Corp.

Dwivedi, P. N., & Upadhyah, S. N. (1977). Particle-fluid mass transfer in fixed and fluidized beds. *Industrial and Engineering Chemistry Process Design and Development, 16*(2), 157.

El-Hisnawi, A. (1981). *Tracer and Reaction Studies in Trickle-Bed Reactors. D.Sc. Thesis*. St. Louis, USA: Washington Univ.

El-Hisnawi, A. A., Dudukovic, M. P., & Mills, P. L. (1982). Trickle-bed reactors: dynamic tracer tests, reaction studies and modelling of reactor performance. *ACS Symposium Series, 196*, 421−440.

Ellman, M. J., Midoux, N., Laurent, A., & Charpentier, J. C. (1988). A new improved pressure drop correlation for trickle bed reactors. *Chemical Engineering Science, 43*, 1677−1684.

Ellman, M. J., Midoux, N., Wild, G., Laurent, A., & Charpentier, J. C. (1990). A new improved liquid hold-up correlation for trickle-bed reactors. *Chemical Engineering Science, 45*, 1677−1684.

Fu, M. S., & Tan, C. S. (1996). Liquid holdup and axial dispersion in trickle-bed reactors. *Chemical Engineering Science, 24*, 5357−5361.

Fukushima, S., & Kusaka, K. (1977a). Interfacial area and boundary of hydrodynamic flow region in packed column with cocurrent downward flow. *Journal of Chemical Engineering of Japan, 10*, 461.

Fukushima, S., & Kusaka, K. (1977b). Liquid-phase volumetric and mass transfer coefficient, and boundary of hydrodynamic flow region in packed column with cocurrent downward flow. *Journal of Chemical Engineering of Japan, 10*, 468.

Germain, A. H., Lefebvre, A. G., L'Homme, G. A. (1974). Experimental study of a catalytic trickle-bed reactor. In, Chemical Reaction Engineering II, Advances in Chemistry Series No. 133, ACS, 164 (Chapter 13).

Gianetto, A., Baldi, G., & Specchia, V. (1970). Absorption in packed towers with concurrent high velocity flows: interfacial areas. *Quaderni Dell Ingegnere Chimico Italino, 6*, 125.

Gianetto, A., Specchia, V., & Baldi, G. (1973). Absorption in packed towers with concurrent downward high velocity flows − II: mass transfer. *AIChE Journal, 19*, 916.

Goto, S., & Smith, J. M. (1975). Trickle-bed reactor performance: I − holdup and mass transfer effects. *AIChE Journal, 21*, 706.

Grosser, K., Carbonell, R. G., & Sundaresan, S. (1988). Onset of pulsing in two-phase cocurrent downflow through a packed bed. *AIChE Journal, 34*, 1850−1860.

Gunjal, P. R., Ranade, V. V., & Chaudhuri, R. V. (2003). Liquid-phase residence time distribution in trickle bed reactors: experiments and CFD simulations. *The Canadian Journal of Chemical Engineering, 81*, 821.

Gunjal, P. R., Kashid, M. N., Ranade, V. V., & Chaudhuri, R. V. (2005). Hydrodynamics of trickle bed reactors: experiments and CFD modeling. *Industrial and Engineering Chemistry Research, 44*, 6278−6294.

Hanika, J. (1999). Safe operation and control of trickle-bed reactor. *Chemical Engineering Science, 54*, 4653−4659.

Hashimoto, K., Muroyama, K., Fujiyoshi, K., & Nagata, S. (1976). Effective radial thermal conductivity in cocurrent flow of a gas and liquid through a packed bed. *International Chemical Engineering, 16*, 720−727.

Herskowitz, M., Carbonell, R. G., & Smith, J. M. (1979). Effectiveness factors and mass transfer in trickle-bed reactors. *AIChE Journal, 25*, 272.

Herskowitz, M., & Smith, J. M. (1983). Trickle bed reactors a review. *AIChE Journal, 29*, 1.

Highfill, W., & Al-Dahhan, M. (2001). Liquid−solid mass transfer coefficient in high pressure trickle bed reactors. *Chemical Engineering Research and Design, 79*, 631.

Hirose, T., Mori, Y., & Sato, Y. (1976). Liquid-to-particle mass transfer in fixed bed reactor with cocurrent gas−liquid flow. *Journal of Chemical Engineering of Japan, 9*, 220.

Hochman, J. M., & Effron, E. (1969). Two-phase cocurrent downflow in packed beds. *Industrial and Engineering Chemistry Fundamentals., 8*, 63.

Holub, R. A., Dudukovic, M. P., & Ramachandran, P. A. (1992). A phenomenological model for pressure drop, liquid holdup, and flow regime transition in gas−liquid trickle flow. *Chemical Engineering Science, 47*, 2343−2348.

Holub, R. A., Dudukovic, M. P., & Ramachandran, P. A. (1993). Pressure drop, liquid holdup, and flow regime transition in trickle flow. *AIChE Journal, 39*, 302−321.

Huang, X., Varma, A., & McCready, M. J. (2004). Heat transfer characterization of gas−liquid flows in a trickle-bed. *Chemical Engineering Science, 59*, 3767−3776.

Iliuta, I., & Larachi, F. (1999). The generalized slit model: pressure gradient, liquid holdup and wetting efficiency in gas−liquid trickle flow. *Chemical Engineering Science, 54*, 5039−5045.

Iliuta, I., & Thyrion, F. C. (1997). Gas−liquid mass transfer in fixed beds with two-phase cocurrent downflow: gas Newtonian and non-Newtonian liquid systems. *Chemical Engineering and Technology, 20*, 538−549.

Iliuta, I., Thyrion, F. C., & Muntean, O. (1996). Hydrodynamic characteristics of two-phase flow through fixed beds: air/Newtonian and non-Newtonian liquids. *Chemical Engineering Science, 51*, 4987−4995.

Jaffe, S. B. (1976). Hot spot simulation in commercial hydrogenation processes. *Industrial and Engineering Chemistry Process Design and Development, 15*, 410−416.

Jolls, K. R., & Hanratty, T. J. (1966). Transition to turbulence for flow through a dumped bed of spheres. *Chemical Engineering Science, 21*, 1185−1190.

Julcour-Lebigue, C., Baussaron, L., Delmas, H., & Wilhelm, A. (2007). Theoretical analysis of tracer method for the measurement of wetting efficiency. *Chemical Engineering Science, 62* (18−29), 5374.

Kan, K. M., & Greenfield, P. F. (1979). Pressure drop and holdup in two-phase cocurrent trickle flows through beds of small particles. *Industrial and Engineering Chemistry Process Design and Development, 18*, 760.

Kawase, Y., & Ulbrecht, J. (1981). Newtonian fluid sphere with rigid or mobile interface in a shear thinning liquid drag and mass transfer. *Chemical Engineering Communications, 8*, 213−228.

Kobayashi, S., Kushiyama, S., Ida, Y., & Wakao, W. (1979). Flow characteristics and axial dispersion in two-phase downflow in packed columns. *Kagaku Kogaku Ronbunshu, 5*, 256.

Krieg, D. A., Helwick, J. A., Dillon, P. O., & McCready, M. J. (1995). Origin of disturbances in cocurrent gas−liquid packed bed flows. *AIChE Journal, 41*, 1653−1666.

Lakota, A., & Levec, J. (1990). Solid−liquid mass transfer in packed beds with cocurrent downward two-phase flow. *AIChE Journal, 36*, 1444.

Lamine, A. S., Gerth, L., Legall, H., & Wild, G. (1996). Heat transfer in a packed bed reactor with cocurrent down flow of a gas and a liquid. *Chemical Engineering Science, 51*(5), 3813−3827.

Lange, R. (1978). *Beitrag zur experimentellen Untersuchung und Modellierung von Teilprozessen für katalytische Dreiphasenreaktionen im Rieselbettreaktor. Ph.D. Thesis*. Germany: Technical University of Leuna-Merseburg.

Larachi, F., Cassanello, M., & Laurent, A. (1998). Gas−liquid interfacial mass transfer in trickle-bed reactors at elevated pressures. *Industrial and Engineering Chemistry Research, 37*, 718−733.

Larachi, F., Laurent, A., Midoux, N., & Wild, G. (1991). Experimental study of a trickle-bed reactor operating at high pressure: two-phase pressure drop and liquid saturation. *Chemical Engineering Science, 46*, 1233−1246.

Larachi, F., Laurent, A., Wild, G., & Midoux, N. (1993). Effect of pressure on the trickle-pulsed transition in irrigated fixed bed catalytic reactors. *Canadian Journal of Chemical Engineering, 71*, 319.

Latifi., M. A., Laurent, A., & Storck, A. (1988). Liquid−solid mass transfer in a packed bed with downward cocurrent gas−liquid flow: an organic liquid phase with high Schmidt number. *Chemical Engineering Journal, 34*, 47.

Latifi, M. A., Midoux, N., Storck, A., & Gence, J. M. (1989). The use of microelectrodes in the study of flow regimes in a packed bed reactor with single phase liquid flow. *Chemical Engineering Science, 44*, 2501−2508.

Latifi, M. A., Naderifar, A., Midoux, N., & Le Mehaute, A. (1994). Fractal behavior of local liquid−solid mass transfer fluctuation at the wall of a trickle bed reactor. *Chemical Engineering Science, 49*, 3823−3829.

Llano, J. J., Rosal, R., Sastre, H., & Díez, F. V. (1997). Determination of wetting efficiency in trickle-bed reactors by a reaction method. *Industrial and Engineering Chemistry Research, 36*, 2616−2625.

Lutran, P. G., Ng, K. M., & Delikat, E. P. (1991). Liquid distribution in trickle beds. An experimental study using computer-assisted tomography. *Industrial and Engineering Chemistry Research, 30*, 1270−1280.

Marcandelli, C., Wild, G., Lamine, A. S., & Bernard, J. R. (1999). Measurement of local particle−fluid heat transfer coefficient in trickle-bed reactors. *Chemical Engineering Science, 54*, 4997−5002.

Matsuura, A., Hitaka, Y., Akehata, T., & Shirai, T. (1979). Effective radial thermal conductivity in packed beds with downward cocurrent gas−liquid flow. *Heat Transfer Japanese Research, 8*, 44−52.

Matsuura, Akinori, Takashi, Akehata, & Takashi, Shirai (1976). Axial dispersion of liquid in concurrent gas−liquid downflow in packed beds. *Journal of Chemical Engineering of Japan, 9*(4), 294−301.

Mears, D. E. (1971). The role of axial dispersion in trickle flow laboratory reactions. *Chemical Engineering Science, 26*, 1361.

Michell, R. W., & Furzer, I. A. (1972). Mixing in trickle flow through packed beds. *Chemical Engineering Journal, 4*, 53.

Midoux, N., Favier, M., & Charpentier, J. C. (1976). Flow pattern, pressure loss and liquid holdup data in gas−liquid downflow packed beds with foaming and nonfoaming hydrocarbons. *Journal of Chemical Engineering of Japan, 9*, 350−356.

Midoux, N., Morsi, B. I., Purwasasmita, M., Laurent, A., & Charpentier, J. C. (1984). Interfacial area and liquid-side mass transfer coefficient in trickle-bed reactors operating with organic liquids. *Chemical Engineering Science, 39*, 781.

Mills, P. L., & Duduković, M. P. (1981). Evaluation of liquid−solid contacting in trickle-bed reactors by tracer methods. *AIChE Journal, 27*, 893−904.

Morsi, B. I., Midoux, N., & Charpentier, J. C. (1978). Flow patterns and some holdup experimental data in trickle-bed reactors for foaming, nonfoaming and viscous organic liquids. *AIChE Journal, 24*, 357−360.

Morsi, B. I., Midoux, N., Laurent, A., & Charpentier, J. C. (1982). Hydrodynamics and interfacial areas in downward cocurrent gas−liquid flow through fixed beds: influence of the nature of the liquid. *International Chemical Engineering, 22*, 142−151.

Muroyama, K., Hashimoto, K., & Tomita, T. (1977). Heat transfer from the wall in gas−liquid cocurrent packed beds. *Kagaku Kogaku Ronbunshu, 3*, 612−616.

Nelson, P. A., & Galloway, T. R. (1975). Particle-to-fluid heat and mass transfer in dense systems of fine particles. *Chemical Engineering Science, 30*, ll−16.

Ng, K. M. (1986). A model for regime transitions in cocurrent down-flow trickle-bed reactors. *AIChE Journal, 32*, 115−122.

Otake, T., & Kunugita, E. (1958). Mixing characteristics of irrigated packed towers. *Chem. Eng. Japan., 22*, 144−150.

Pant, H. J., Saroha, A.K, & Nigam, K. D. P. (2000). Measurement of liquid holdup and axial dispersion in trickle bed reactors using radiotracer technique. *NUKLEONIK, 45*(4), 235−241.

Ramachandran, P. A., & Smith, J. M. (1979). Mixing-cell method for design of trickle-bed reactors. *Chemical Engineering Journal, 17*(2), 91−99.

Ranz, W. E. (1952). Friction and heat transfer co-efficient for single particles and packed beds. *Chemical Engineering Progress, 48*(8), 247.

Rao, V. G., Ananth, M. S., & Varma, Y. B. G. (1983). Hydrodynamics of two-phase cocurrent downflow through packed beds (parts I and II). *AIChE Journal, 29*, 467−483.

Rao, V. G., & Drinkenburg, A. A. H. (1985). Solid−liquid mass transfer in packed beds with cocurrent gas−liquid down flow. *AIChE Journal, 31*, 1059.

Ring., Z. E., & Missen, R. W. (1991). Trickle-bed reactors: tracer study of liquid holdup and wetting efficiency at high temperature and pressure. *Canadian Journal of Chemical Engineering, 69*, 1016.

Saez, A. E., & Carbonell, R. G. (1985). Hydrodynamic parameters for gas−liquid cocurrent flow in packed beds. *AIChE Journal, 31*, 52−62.

Sai, P. S. T., & Varma, Y. B. G. (1987). Pressure drop in gas−liquid downflow through packed beds. *AIChE Journal, 33*, 2027−2036.

Sai, P. S. T., & Varma, Y. B. G. (1988). Flow pattern of the phases and liquid saturation in gas−liquid cocurrent downflow through packed beds. *Canadian Journal of Chemical Engineering, 66*, 353−360.

Saroha, A. K., & Nigam, K. D. P. (1996). Trickle bed reactor. *Reviews in Chemical Engineering, 12*(3), 207−346.

Saroha, A. K., Nigam, K. D. P., Saxena, A. K., & Kapoor, V. K. (1998). Liquid distribution in trickle-bed reactors. *AIChE Journal, 44*, 2044−2052.

Satterfield, C. N. (1975). Trickle bed reactors. *AIChE Journal, 21*, 209−228.

Satterfield, C. N., Van Eek, M. W., & Bliss, G. S. (1978). Liquid-solid mass transfer in Packed Beds with downward concurrent gas-liquid flow. *AIChE J., 24*, 709.

Scheidegger, A. E. (1974). *The Physics of Flow through Porous Media* (3rd ed.). univ. de Toronto Press.

Schwartz, J. G., Weger, E., & Dudukovic, M. P. (1976). A new tracer method for determination of solid−liquid contacting efficiency in trickle-bed reactors. *AIChE Journal, 22*, 894.

Sederman, A. J., & Gladden, L. F. (2001). Magnetic resonance imaging as a quantitative probe of gas−liquid distribution and wetting efficiency in trickle-bed reactors. *Chemical Engineering Science, 56*, 2615−2628.

Seguin, D., Montillet, A., & Comiti, J. (1998). Experimental characterization of flow regimes in various porous media − I: limit of laminar flow regime. *Chemical Engineering Science, 53*(21), 3751.

Seguin, D., Montillet, A., Comiti, J., & Huet, F. (1998). Experimental characterization of flow regimes in various porous media − II: transition to turbulent regime. *Chemical Engineering Science, 53*, 3897−3909.

Sicardi, S., Gerhard, H., & Hofmann, H. (1979). Flow regime transition in trickle-bed reactors. *Chemical Engineering Journal, 18*, 173−182.

Sicardi, S., & Hofmann, H. (1980). Influence of gas velocity and packing geometry on pulsing inception in trickle bed reactors. *Chemical Engineering Journal, 20*, 251−253.

Sie, S. T., & Krishna, R. (1998). Process development and scale up − III. Scale-up and scale-down of trickle bed processes. *Reviews in Chemical Engineering, 14*, 203.

Specchia, V., & Baldi, G. (1977). Pressure drop and liquid holdup for two phase concurrent flow in packed beds. *Chemical Engineering Science, 32*, 515−523.

Specchia, V., & Baldi, G. (1979). Heat transfer in trickle-bed reactors. *Chemical Engineering Communications, 3*, 483−499.

Specchia, V., Baldi, G., & Gianetto, A. (1978). Solid−liquid mass transfer in concurrent two-phase flow through packed beds. *Industrial and Engineering Chemistry Process Design and Development, 17*, 362.

Talmor, E. (1977). Two-phase downflow through catalyst beds. Parts I and II. *AIChE Journal, 23*, 868−878.

Tan, C. S., & Smith, J. M. (1982). A dynamic method for liquid-solid mass transfer in Trickle Beds. *AIChE J., 28*, 190.

Tosun, G. (1982). Axial *dispersion* in trickle bed reactors: influence of the gas flow rate. *Industrial and Engineering Chemistry Fundamentals, 21*, 184−186.

Tsochatzidis, N. A., & Karabelas, A. J. (1994). Study of pulsing flow in a trickle bed using the electro-diffusion technique. *Journal of Applied Electrochemistry, 24*, 670−675.

Turek, F., Lange, R., & Bush, A. (1979). *Chemie Technik., 31*, 232.

Van Swaaij, W. P. M., Charpentier, J. C., & Villermaux, J. (1969). Residence time distribution in the liquid phase of trickle flow in packed columns. *Chemical Engineering Science, 24*, 1083.

Wammes, W. J. A., & Westerterp, K. R. (1990). The influence of reactor pressure on the hydrodynamics in a cocurrent gas−liquid trickle-bed reactor. *Chemical Engineering Science, 45*, 2247−2254.

Wammes, W. J. A., & Westerterp, K. R. (1991). Hydrodynamics in a pressurized cocurrent gas−liquid trickle-bed reactor. *Chemical Engineering Technology, 14*, 406.

Wanchoo, R. K., Kaur, N., & Bansal, M. (2007). RTD in trickle-bed reactors: experimental study. *Chemical Engineering Communications, 194*(1503), 50−68.

Wang, Y., Mao, Z., & Chen, J. (1998). A new instrumentation for measuring the small scale maldistribution of liquid flow in trickle beds. *Chemical Engineering Communications, 163*, 233−244.

Weekman, V. W. (1976). Hydroprocessing reaction engineering. In *Proceedings of the fourth international/sixth European symposium on chemical reaction engineering*. Heidelberg, Germany: VDI.

Weekman, V. W., & Myers, J. E. (1964). Fluid-flow characteristics of concurrent gas−liquid flow in packed beds. *AIChE Journal, 10*, 951−957.

Weekman, V. W., & Myers, J. E. (1965). Heat transfer characteristics of concurrent gas−liquid flow in packed beds. *AIChE Journal, 11*, 13−17.

Wild, G., Larachi, F., & Charpentier, J.-C. (1992). Heat and mass transfer in gas−liquid−solid fixed bed reactors. In M. Quintard, & M. Todorović (Eds.), *Heat and mass transfer in porous media*. Amsterdam, The Netherlands: Elsevier. p. 616.

Wu, Y., Khadilkar, M. R., Al-Dahhan, M. H., & Dudukovic, M. P. (1996). Comparison of upflow and downflow two-phase flow packed bed reactors with and without fines: experimental observations. *Industrial and Engineering Chemical Research, 35*(2), 397−405.